Memorial Sloan Kettering Cancer Center

Leveraging Cancer Metabolism

Kayvan R. Keshari, PhD
www.ski.edu/keshari
@KeshariLab

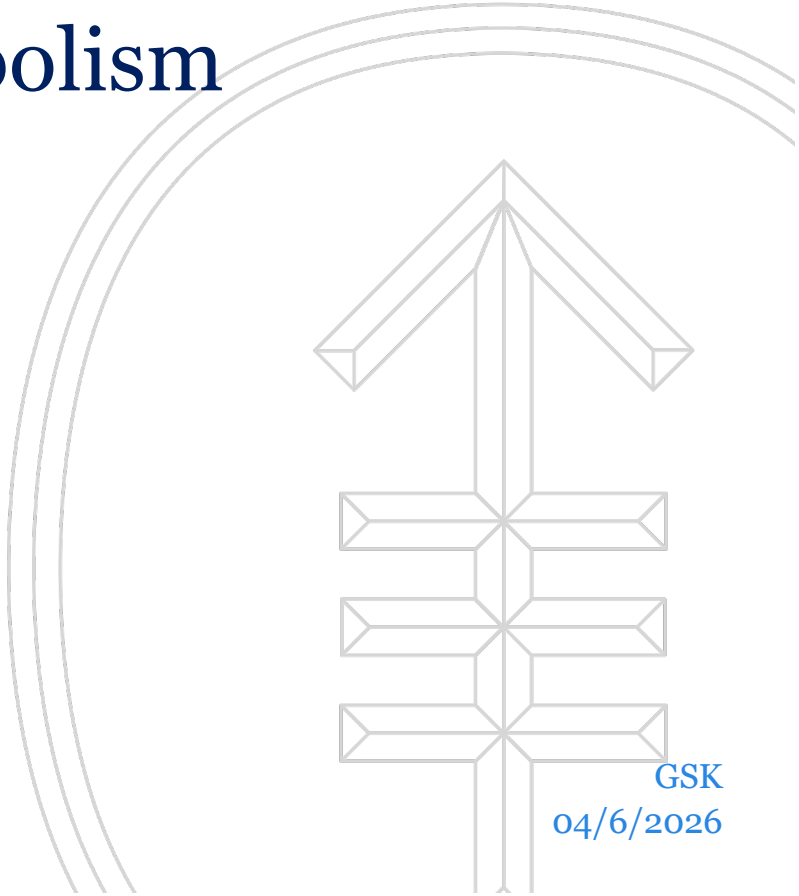

GSK
04/6/2026

The Plan

1. Quick introduction to Isotope tracing and Flux analysis

2. Drugging metabolism – targeting key pathways
   a. Glucose metabolism
   b. Glutamine metabolism
   c. Fatty acid metabolism
   d. Nucleotide metabolism

3. Detecting metabolism
   a. Methods - Optical, electrochemical, PET and MRI
   b. What is the difference between uptake, the pool and the flux?

4. Engineering metabolism
   a. Can we manipulate the metabolism of a cell to do what we want?
   b. What can we learn from model organisms?

5. Paper Discussion

References

- Nielsen, J. & Keasling, J. D. **Engineering Cellular Metabolism**. *Cell* 164, 1185-1197, doi:10.1016/j.cell.2016.02.004 (2016).
- Stine, Z. E., Schug, Z. T., Salvino, J. M. & Dang, C. V. **Targeting cancer metabolism in the era of precision oncology.** *Nat Rev Drug Discov* 21, 141-162, doi:10.1038/s41573-021-00339-6 (2022).
- DeBerardinis, R. J. & Keshari, K. R. **Metabolic analysis as a driver for discovery, diagnosis, and therapy.** *Cell* 185, 2678-2689, doi:10.1016/j.cell.2022.06.029 (2022).

Oncogenic signaling is intimately connected to metabolism

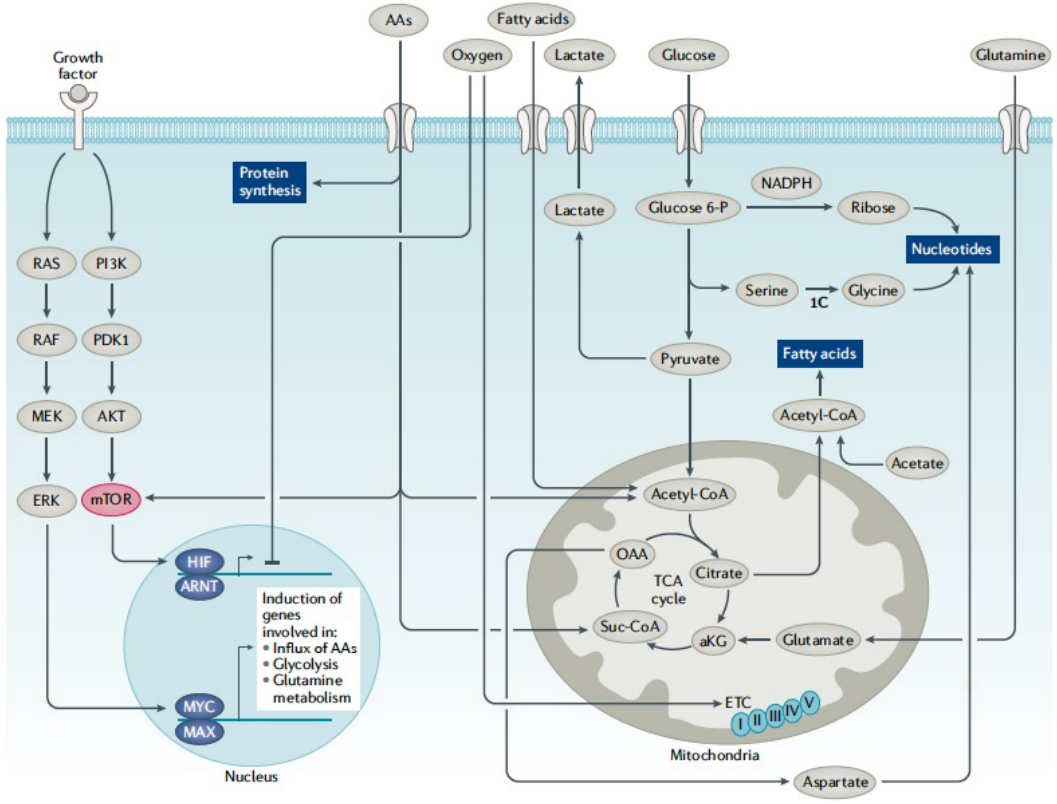

Memorial Sloan Kettering Cancer Center

Isotope Tracing?

Perturbations in metabolite pools are related to key oncogenic drivers

How can we truly annotate these changes?

Isotope tracing is not a new idea…

- Radioactive isotopes were first used in biological systems in the 1920s by George de Hevesy, who won the Nobel Prize in Chemistry in 1943 - Traced using ^{212}Pb into *Vicia faba* (horse-bean)[1]
- Later the first stable isotopes were used for tracing, including ^{2}H tracing by Schoenheimer[2]
- This lead to isolated organs, particularly the heart, and to translate isotopic labeling data into relative or absolute metabolic fluxes[3]
- Used in humans since 1934, when Hevesy and Hofer used deuterium oxide to estimate the size of the whole-body water pool and rate of water elimination[4]

[1]Hevesy Biochem J 1923
[2]Schoenheimer et al. *Science* 1935, *J Biochem* 1936
[3]Chance et al. 1983, Malloy et al. 1987, Russel et al 1997
[4]Hevesy and Hofer *Nature* 1934

Isotope Tracing – how do we do it?

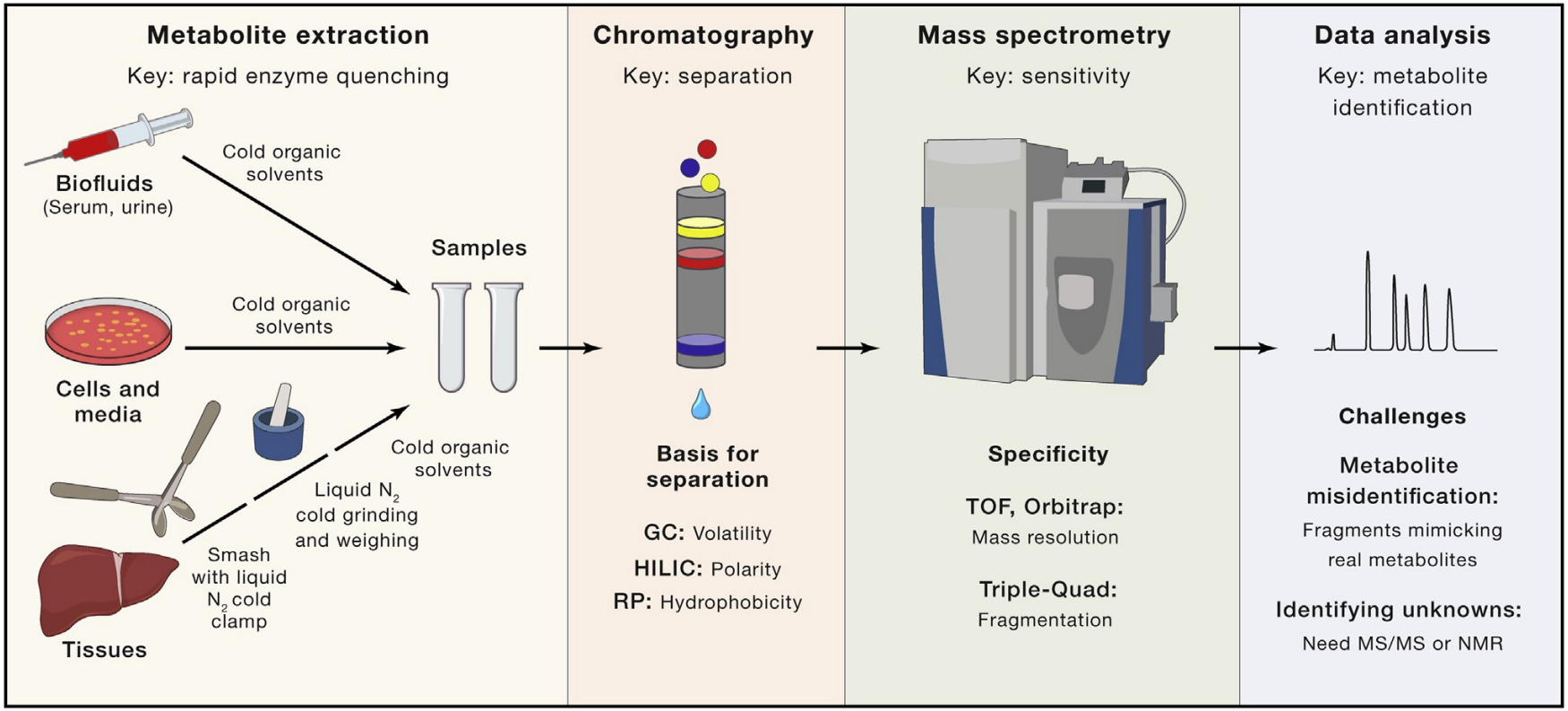

Jang *Cell* 2018

Memorial Sloan Kettering Cancer Center

Pool size versus Flux

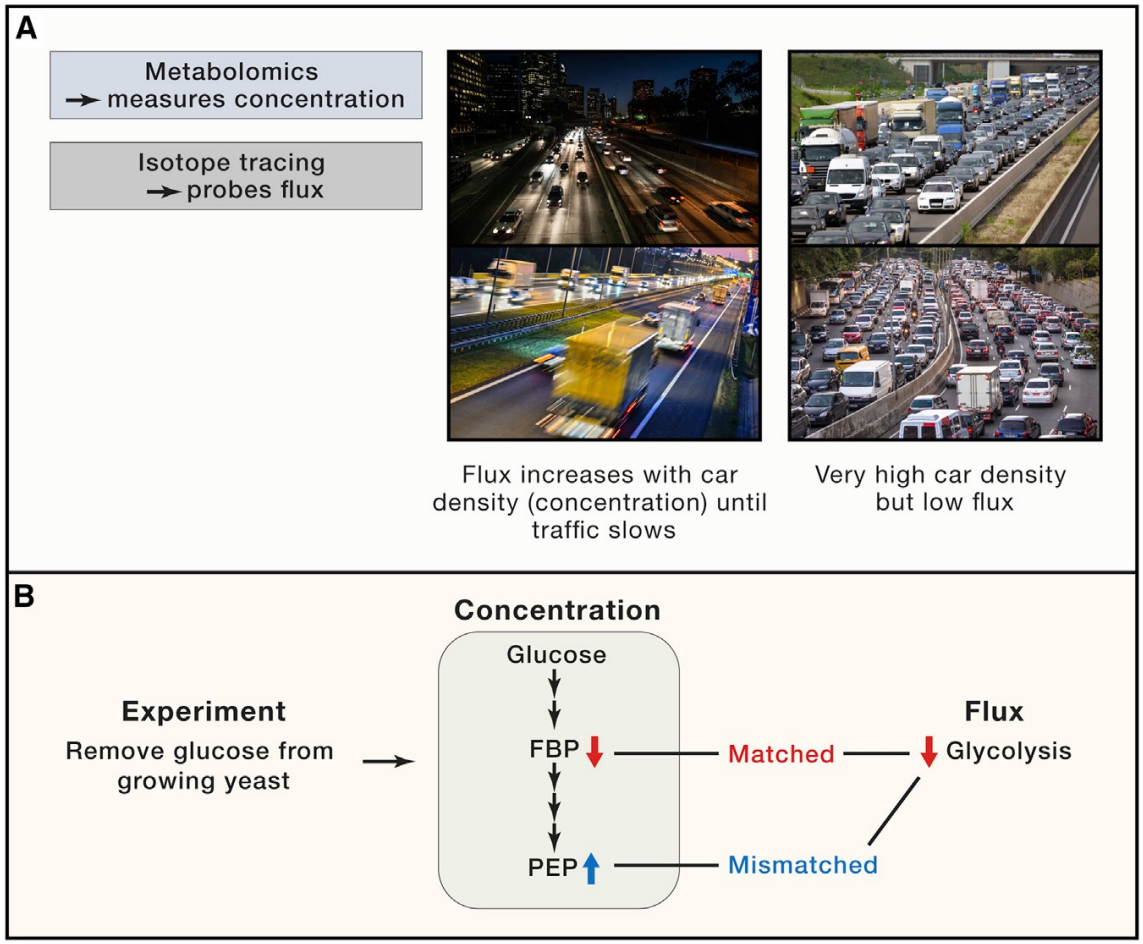

Memorial Sloan Kettering Cancer Center

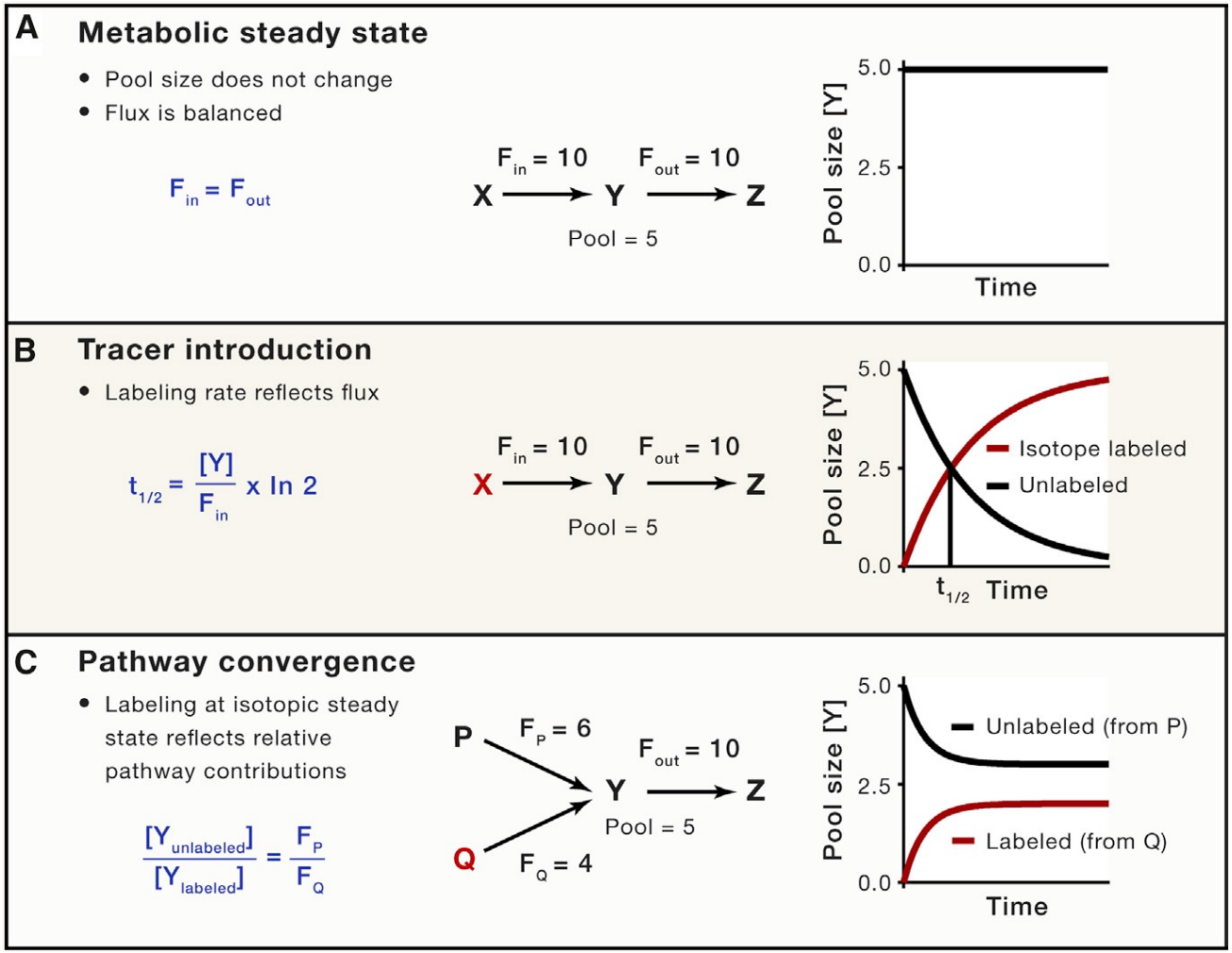

Stable isotopes can probe many metabolic pathways in many organs and physiological states

- A systematic analysis of nutrient turnover in mice, (steady-state infusion of over 30 nutrients), revealed a high contribution of lactate to the TCA cycle, exceeding glucose's contribution in most tissues (Hui et al., 2017)
  - Confirmed in pigs through assessment of organ-specific metabolite consumption and production (Jang et al., 2019).
- Unexpected aspects of metabolic regulation in mice revealed by isotope tracing -
  - Glycogen contributes to glycolytic flux in many organs in the fed state (TeSlaa et al., 2021), contrasting with the common perception that glycogenolysis is restricted to a few tissues during fasting
  - Hepatic fat production (in mice) for hepatic lipogenesis arises from acetate derived from dietary fructose through the activity of intestinal flora, and NADPH for this process arises from folate metabolism rather than the pentose phosphate pathway (Zhang et al., 2021; Zhao et al., 2020)
- In rats, the importance of PEP cycling in pancreatic beta cells and liver to maintain glucose homeostasis and reduce hepatic fat content (Abulizi et al., 2020).

How would you use it to parse metabolism *in vivo*

Orthotopic patient-derived glioma xenografts, steady-state infusions of [U-^{13}C]glucose revealed glycolysis, glucose oxidation in the TCA cycle, glutamine synthesis and other pathways in the tumors, and identified conserved metabolic features among xenografts from different patients (Marin-Valencia et al., 2012).

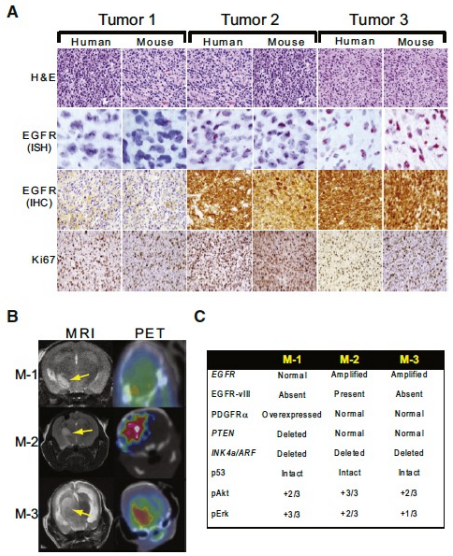

	M-1	M-2	M-3
EGFR	Normal	Amplified	Amplified
EGFR-vIII	Absent	Present	Absent
PDGFRα	Overexpressed	Normal	Normal
PTEN	Deleted	Normal	Normal
INK4a/ARF	Deleted	Deleted	Deleted
p53	Intact	Intact	Intact
pAkt	+2/3	+3/3	+2/3
pErk	+3/3	+2/3	+1/3

Figure 1. Human Orthotopic Tumors Established from Three Primary Human GBMs

(A) Hematoxylin and eosin (H&E) stains, *EGFR* in situ hybridization (ISH) and immunohistochemistry (IHC), and Ki67 staining of parental human GBMs and representative mouse HOTs.

(B) MRI and ^{18}FDG-PET of representative mouse HOTs (M-1, M-2, M-3) derived from each parental line. Arrows indicate GBM masses in the right hemisphere.

(C) Summary of genomic and IHC data from HOTs M-1, M-2, and M-3.

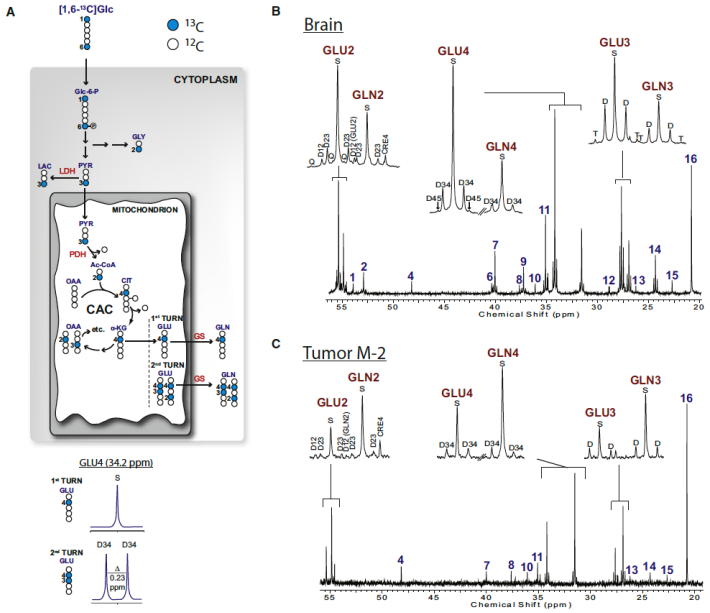

Figure 3. Metabolism of [1,6-^{13}C]Glucose in HOTs and Surrounding Brain

(A) Illustration of [1,6-^{13}C]glucose metabolism. Filled symbols are ^{13}C and open symbols are ^{12}C. The diagram shows the positions of ^{13}C after glucose is metabolized through glycolysis, glycine synthesis, and multiple turns of the CAC. Numbers refer to carbon positions. At the bottom, the spectra demonstrate the appearance of the ^{13}C NMR spectra for glutamate labeled in position 4 alone (S, singlet), or in positions 3 and 4 (D34, 3-4 doublet), as detailed in Supplemental Experimental Procedures. Abbreviations: Glc, glucose; Glc-6-P, glucose-6-phosphate; GLY, glycine; PYR, pyruvate; LAC, lactate; Ac-CoA, acetyl-CoA; CIT, citrate; α-KG, α-ketoglutarate; OAA, oxaloacetic acid; GLU, glutamate; GLN, glutamine; LDH, lactate dehydrogenase; PDH, pyruvate dehydrogenase; GS, glutamine synthetase.

(B and C) Brain (B) and tumor (C) spectra from a mouse with an M-2 HOT infused with [1,6-^{13}C]glucose. Insets are GLU and GLN C2, C3, and C4. Chemical shift assignments are the same for all spectra in the paper: *1*, NAA C2; *2*, Aspartate C2; *3*, Alanine C2; *4*, Taurine C1; *5*, Glycine C2; *6*, NAA C3; *7*, GABA C4; *8*, Creatine C2; *9*, Aspartate C3; *10*, Taurine C2; *11*, GABA C2; *12* and *13*, unassigned; *14*, GABA C3; *15*, NAA C6; *16*, Lactate C3. Abbreviations: S, singlet; D, doublet; T, triplet; Q, quartet; ppm, parts per million.

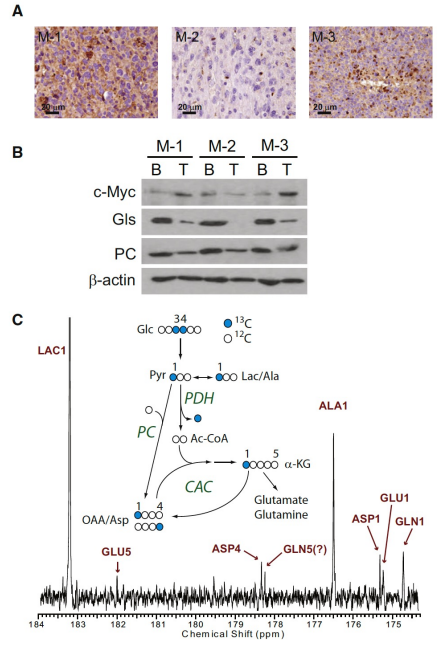

Figure 5. Anaplerosis in HOTs

(A) c-Myc IHC in HOT tumors.

(B) Protein abundance of c-Myc and two anaplerotic enzymes, glutaminase (GLS), and pyruvate carboxylase (PC) in HOT tumors (T) and surrounding brain (B).

(C) ^{13}C NMR spectrum from an M-1 tumor infused with [3,4-^{13}C]glucose. The diagram illustrates that in this infusion, PC is active if C1 signal exceeds C5 signal in glutamate and glutamine. GLN5 was not definitively assigned; it is either the indicated peak or coresonant with ASP4, both of which are smaller than the GLN1 peak.

Isotope tracing with infusions are safe

- Infusions with ^{13}C-glucose are safe and used to probe metabolism in solid tumors of several kinds, including from pediatric patients as young as 4 months (Johnston et al., 2021).
- Adult gliomas and brain metastases, ^{13}C NMR analysis of tumor metabolites revealed that glucose is not only oxidized in the TCA cycle, but also provides a carbon source for anaplerosis (Maher et al., 2012)
- A surprising finding of that study was the low fraction of acetyl-CoA produced from glucose
  - This prompted exploration for other respiratory substrates and revealed that acetate can also be taken up by these tumors, converted to acetyl-CoA and used to feed the TCA cycle (Mashimo et al., 2014)
  - In triple negative breast cancer, glucose supplies glycolysis, the pentose phosphate pathway, the TCA cycle and nonessential amino acid synthesis (Ghergurovich et al., 2021)
- Suppression of TCA cycle metabolism in clear cell renal cell carcinomas relative to nonmalignant kidney (Courtney et al., 2018)
- Probe T cell subsets after physiological stimulation *in vivo* (Ma et al., 2019).
- It is also possible to assess metabolism in utero by infusing ^{13}C-glucose, ^{13}C-glutamine and other tracers into pregnant mice at the desired gestational age (Solmonson et al., 2022).

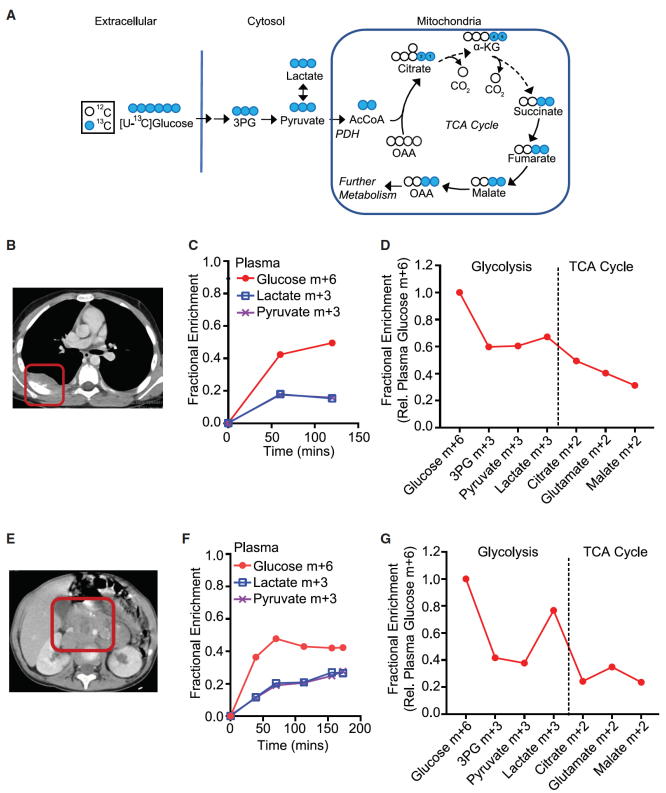

Figure 2. ^{13}C labeling in tumor metabolites from two children with neuroblastomas
(A) Expected labeling of glycolytic and TCA cycle metabolites after infusion with [U-^{13}C]glucose. In this scheme, the 2 labeled carbons from acetyl-CoA are transferred to citrate positions 1 and 2 and then to positions 4 and 5 of α-ketoglutarate (α-KG) and carried further around the TCA cycle. Labeled OAA exchanges with labeled aspartate. Further metabolism of labeled OAA into subsequent turns of the cycle is not illustrated.
(B) Computed tomography of patient 1, a 9-year-old boy with a non-*MYCN*-amplified neuroblastoma (red box).
(C) Time-dependent labeling of glucose, lactate, and pyruvate in patient 1's plasma during the [U-^{13}C]glucose infusion.
(D) Labeling in metabolites extracted from patient 1's tumor. Labeling is normalized to the glucose m+6 fraction in plasma at the time of tumor resection.
(E) Computed tomography of patient 3, a 2-year-old girl with a non-*MYCN*-amplified neuroblastoma (red box).
(F) Time-dependent labeling of glucose, lactate, and pyruvate in patient 3's plasma during the [U-^{13}C]glucose infusion.
(G) Labeling in metabolites extracted from patient 3's tumor. Labeling is normalized to the glucose m+6 fraction in plasma at the time of tumor resection.

Drugging Metabolism – key pathways

- Glucose metabolism
- Glutamine metabolism
- Fatty acid metabolism
- Nucleotide metabolism

Current Cancer Metabolism Targets

Table 1 | **Small molecules that target cancer metabolism**

Agent	Target	Function	Indications
Approved cancer metabolic drugs			
Pemetrexed	TYMS, DHFR	dUMP to dTMP conversion; folate to THF conversion	NSCLC
5-Fluorouracil	TYMS	dUMP to dTMP conversion	CRC, gastric and breast cancer
Hydroxyurea	RNR	Ribonucleotide to deoxyribonucleotide conversion	CML, HNSCC
Gemcitabine	DNA incorporation	Nucleotide analogues	Pancreatic, ovarian and breast cancer; NSCLC
Fludarabine	DNA incorporation	Nucleotide analogues	CLL
6-Mercaptopurine	PPAT	Purine synthesis	ALL
Methotrexate	DHFR	Folate to THF conversion	Breast, HNSCC, lung, non-Hodgkin lymphomas
Enasidenib	Mutant IDH2	2-Hydroxyglutarate synthesis	AML
Ivosidenib	Mutant IDH1	2-Hydroxyglutarate synthesis	AML
Approved metabolic drugs for non-cancer indications			
Metformin	Complex I	Oxidative metabolism	Type 2 diabetes mellitus
Leflunomide	DHODH	Pyrimidine metabolism	Rheumatoid arthritis
Bempedoic acid	ACLY	Lipid synthesis	Heterozygous familial hypercholesterolaemia, established atherosclerotic cardiovascular disease
Hydroxychlorquine	Autophagy	Removal of damaged cellular components	Rheumatoid arthritis
Sulfasalazine	SLC7A11/xCT	Cystine/glutamate exchange	Ulcerative colitis
Small-molecule metabolic inhibitors in cancer clinical trials			
CPI-613	Mitochondria	Oxidative metabolism	Pancreatic cancer, AML, solid tumours, lymphoma
IM156	Mitochondria	Complex I	Solid tumours, lymphoma
IACS-010759	Mitochondria	Complex I	AML, advanced solid tumours
CB-839	Glutaminase	Glutamine to glutamate conversion	Leukaemia, CRC, breast cancer, RCC
IPN60090	Glutaminase	Glutamine to glutamate conversion	Advanced solid tumours
DRP-104	Glutamine-utilizing enzymes	Glutamine-dependent enzymes	NSCLC, NHSCC, advanced solid tumours
AZD-3965	MCT1	Lactate symporter	Advanced cancers
TVB-2640	FASN	Fatty acid synthesis	NSCLC, CRC, breast cancer, astrocytoma
AG-270	MAT2A	Production of S-adenosylmethionine	Advanced solid tumours or lymphoma
SM-88	Tyrosine metabolism	Oxidative stress	Sarcoma, prostate, breast and pancreatic cancer
Indoximod	IDO1	Kynurenine synthesis	Melanoma, breast and pancreatic cancer
Epacadostat	IDO1	Kynurenine synthesis	Breast cancer, HNSCC, NSCLC, melanoma, RCC

Stine et al. *Nat Rev Drug Disc* 2022

Memorial Sloan Kettering Cancer Center

Drugging Metabolism - Glucose

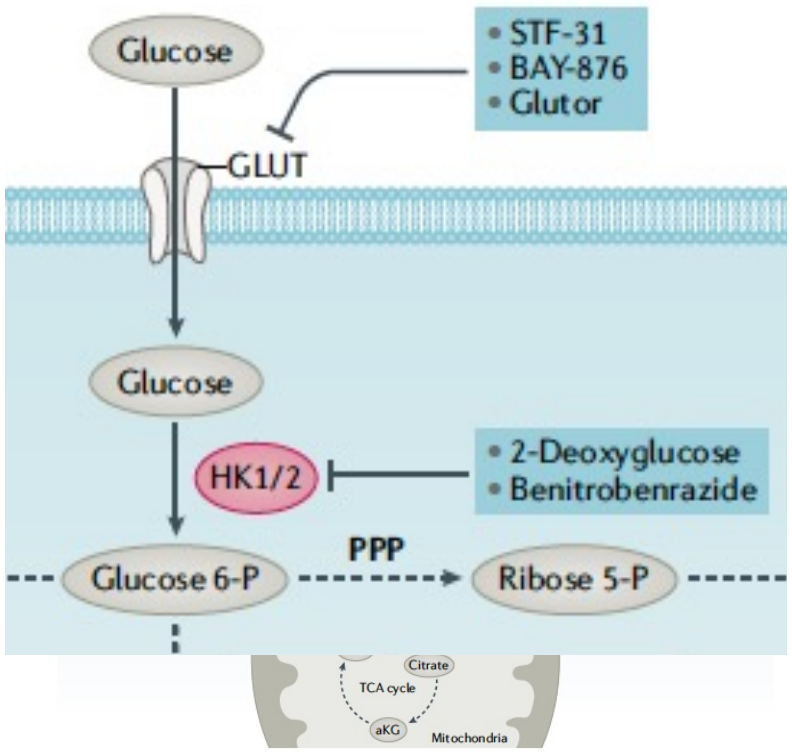

Hexokinase – 2DG

Woodward and Cramer. *J Franklin Ins*
2-Desoxyl-D-glucose as an inhibitor o
tumor tissue

Anaerobic glucose metabolism of slic
carcinoma was found to be inhibited a
equimolar quantity of 2-deoxy-D-gluc

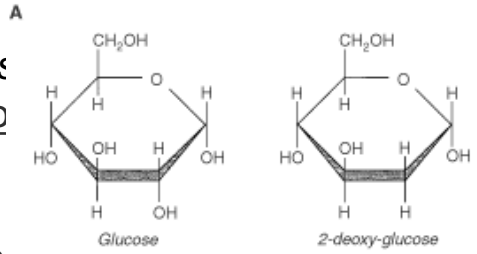

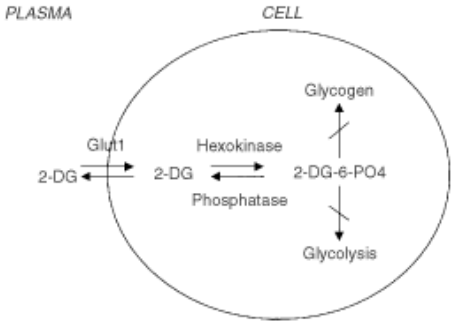

Aft et al. *BJC* 2002

Memorial Sloan Kettering Cancer Center

Drugging Metabolism - Glucose

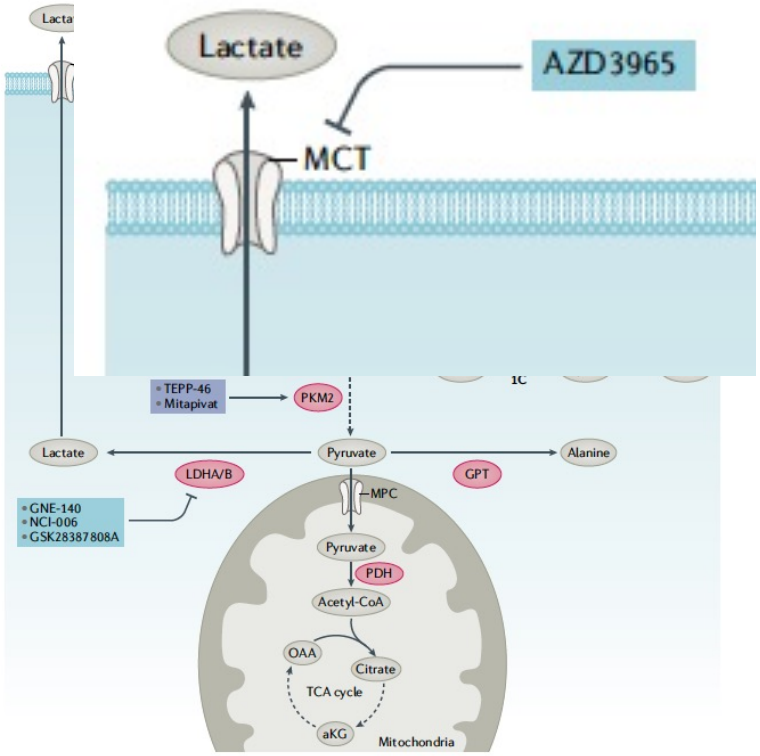

MCT1 inhibitor AZD3965

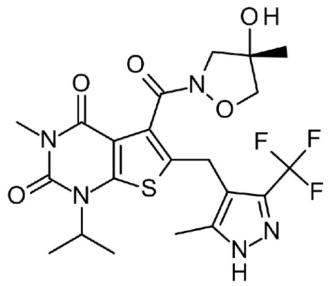

Curtis et al. *Oncotarget* 2017

Pre-clinical pharmacology of AZD3965, a selective inhibitor of MCT1: DLBCL, NHL and B

AZD3965 bound to human MCT1 (pKi 8.8)

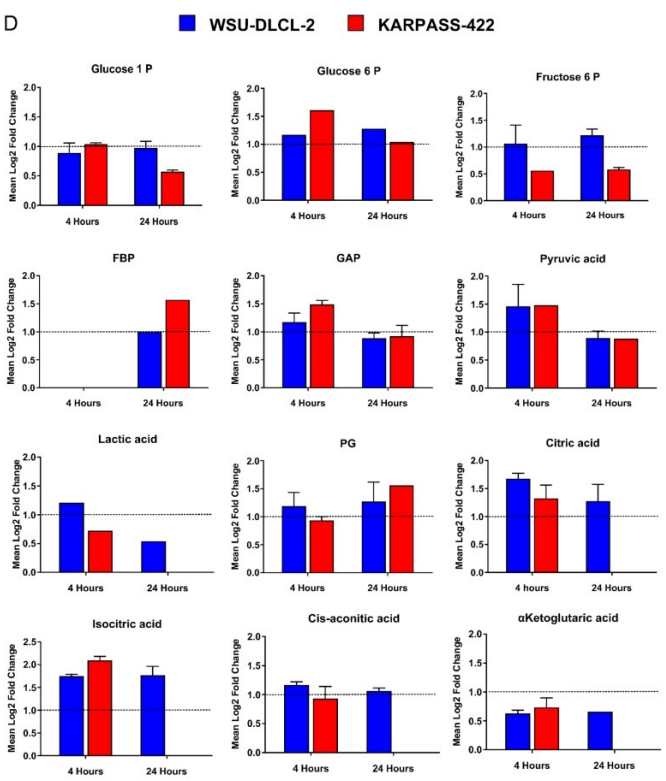

Drugging Metabolism – Glutamine

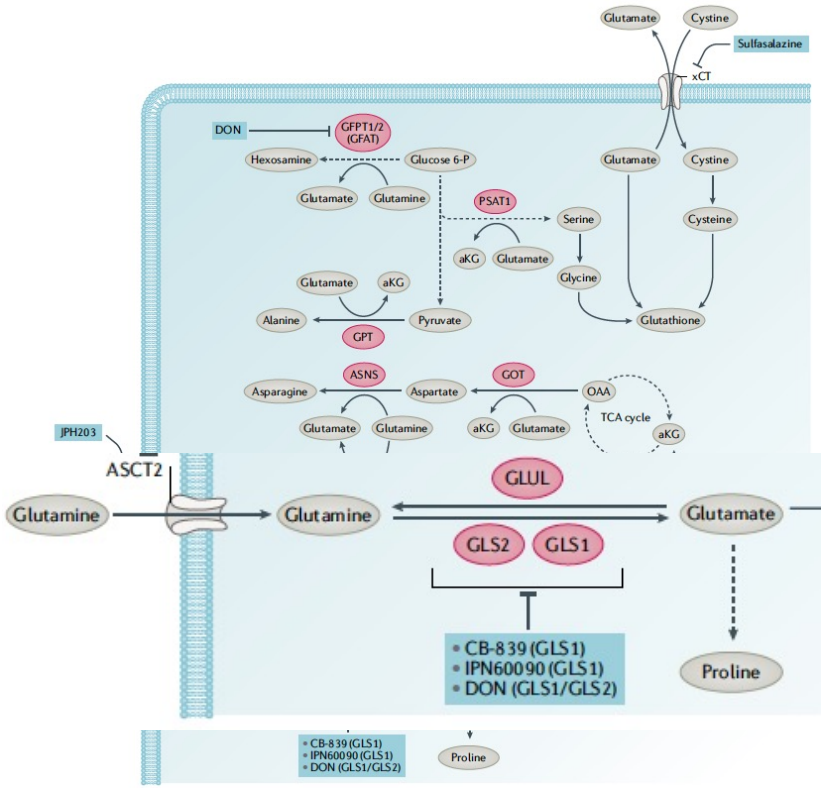

CB-839 – G

Gross et al.
Antitumor A
Triple-Nega

CB-839 beh
impacting W

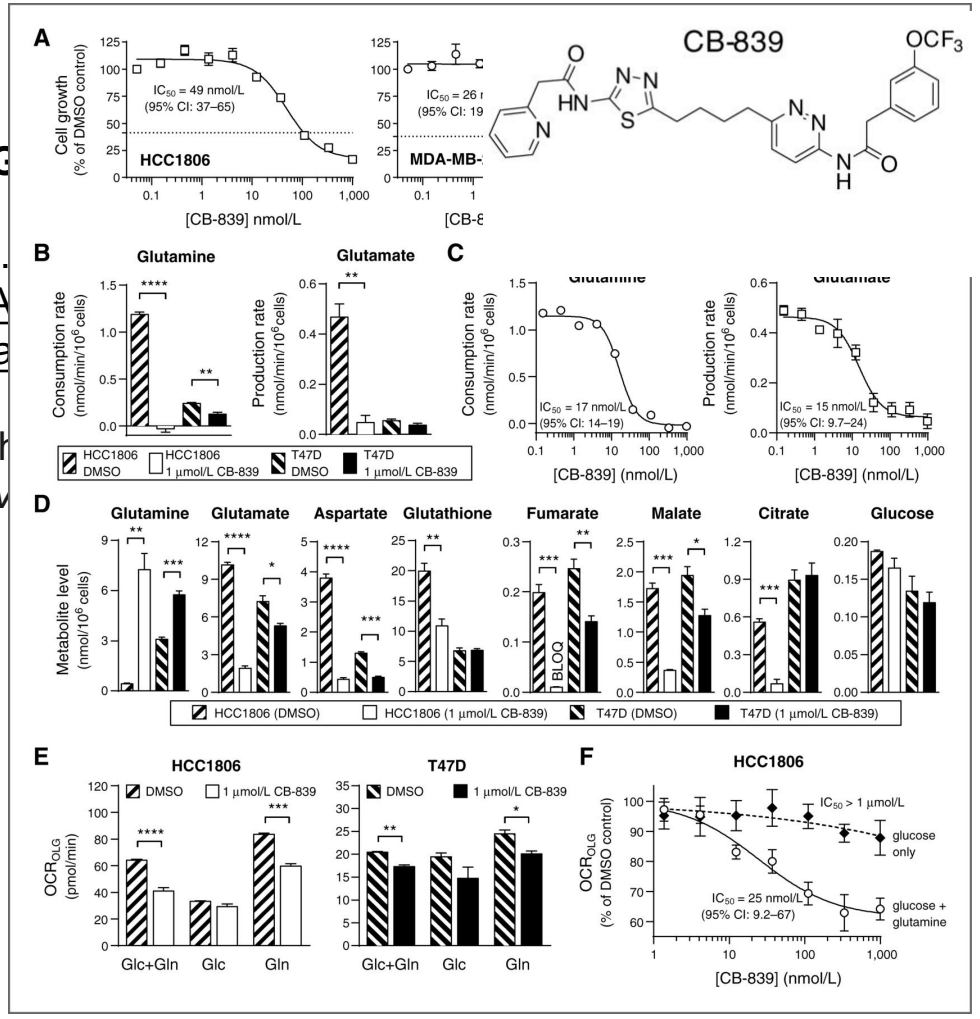

Drugging Metabolism – Glutamine

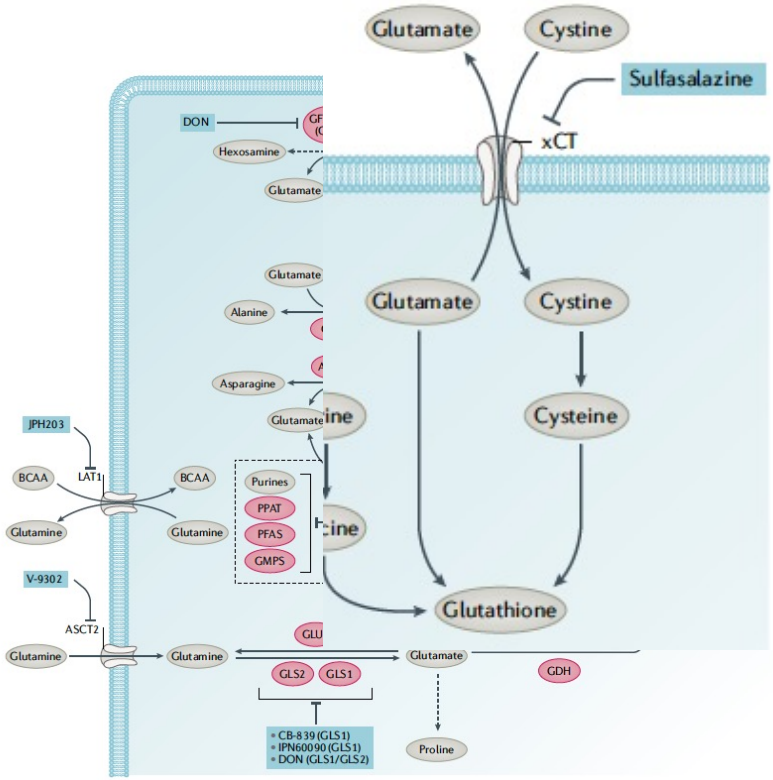

Sulfasalazine – xCTi

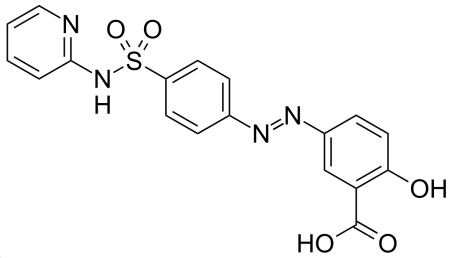

Gout et al. *Leukemia* 2001
Sulfasalazine, a potent suppressor of lymphoma growth by inhibition of the xc − cystine transporter: a new action for an old drug

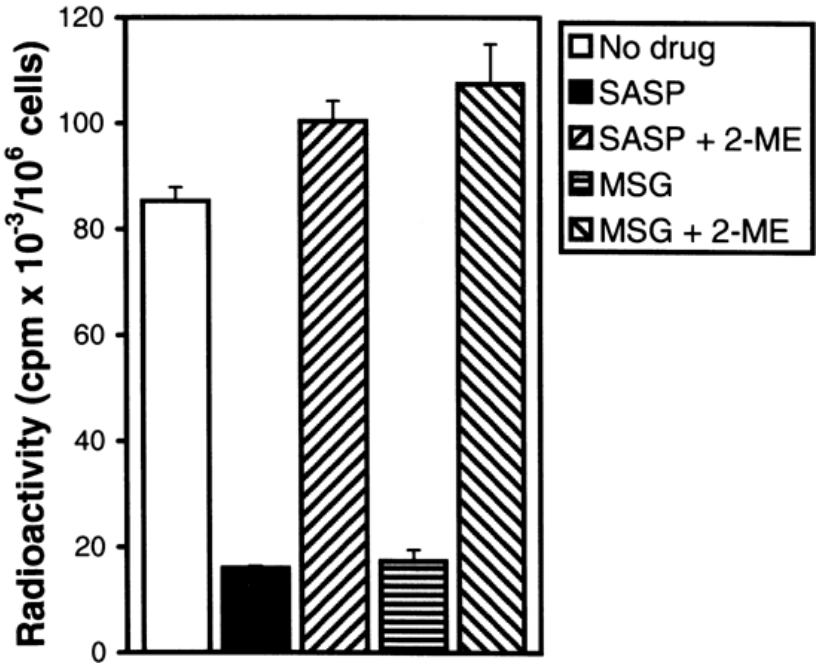

Drugging Metabolism – Fatty Acids

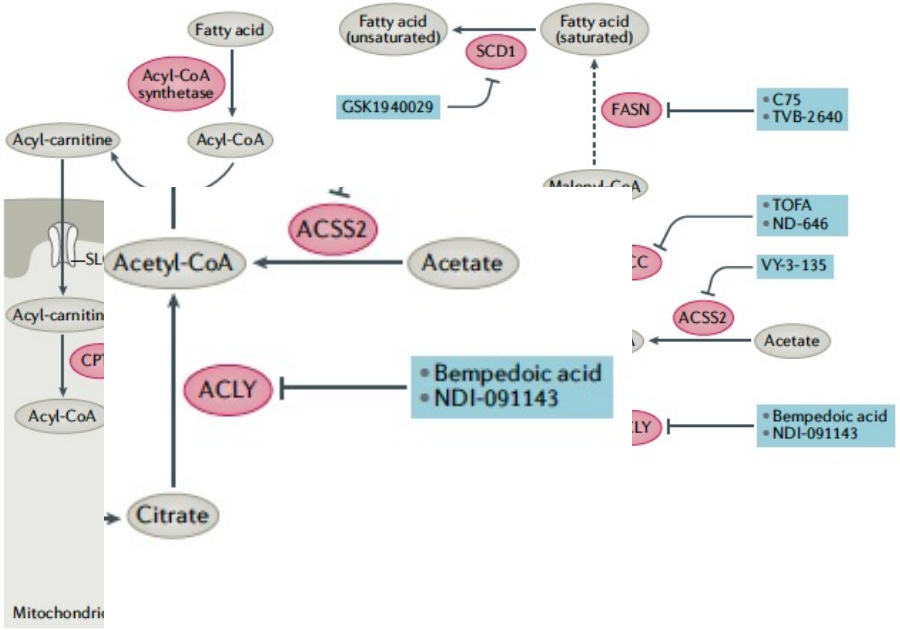

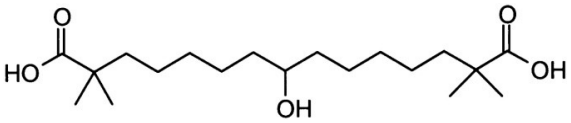

Bempedoic acid – ACLYi

Cramer et al. *JLR* 2004

Effects of a novel dual lipid synthesis inhibitor and its potential utility in syndrome

In Pinkosky - Wh
CoASH concentra
apparent Km for
approximately 4.5
support that ETC
concentrations c
synthesis and tha

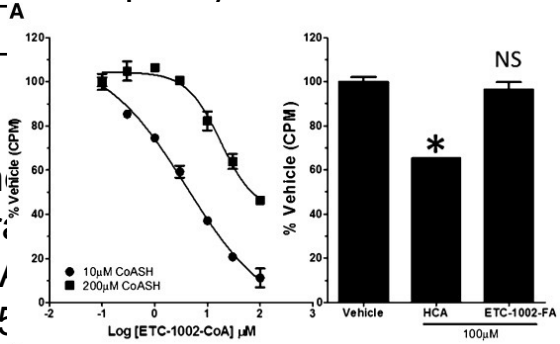

Pinkosky et al. *JLR* 2013

Drugging Metabolism - Nucleotides

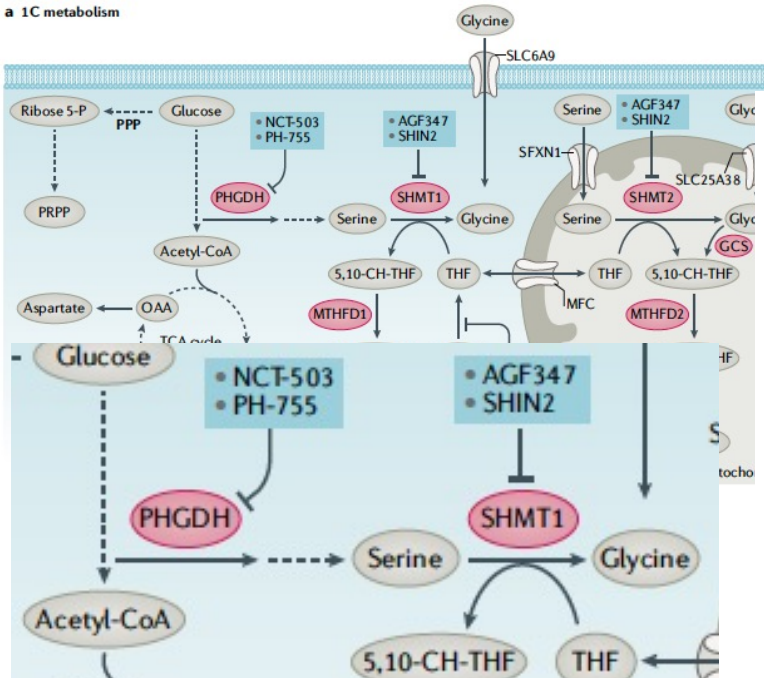

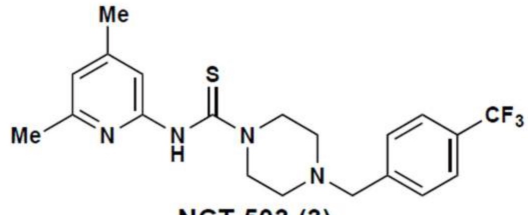

NCT-503 – PHGDHi

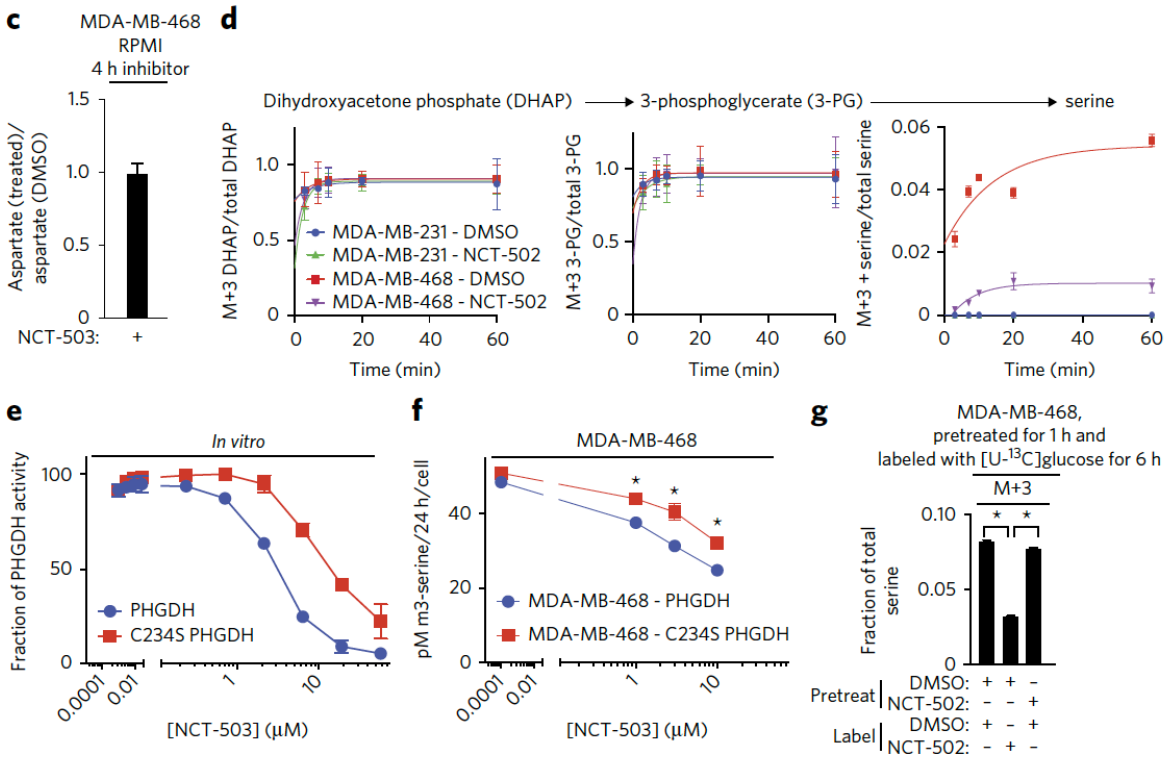

Drugging Metabolism - Nucleotides

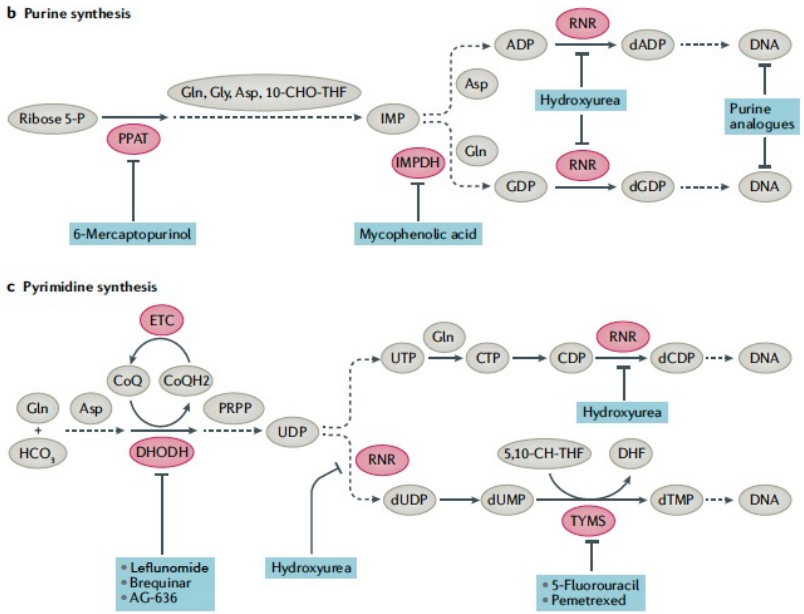

Hydroxyurea – RNRi

Steams et al. *Med. Pharmacol. Chem* 1963 Hydroyxurea: a new type of potential anti-tumor agent.

Shown to inhibit leukemia cell proliferation later shown to inhibit RNR (Slater *JBC* 1973)

Lets take a break

Memorial Sloan Kettering Cancer Center

Detecting Metabolism - Methods

1. Optical
2. Electrochemical
3. PET
4. MRI

Spatial Resolution and targeting

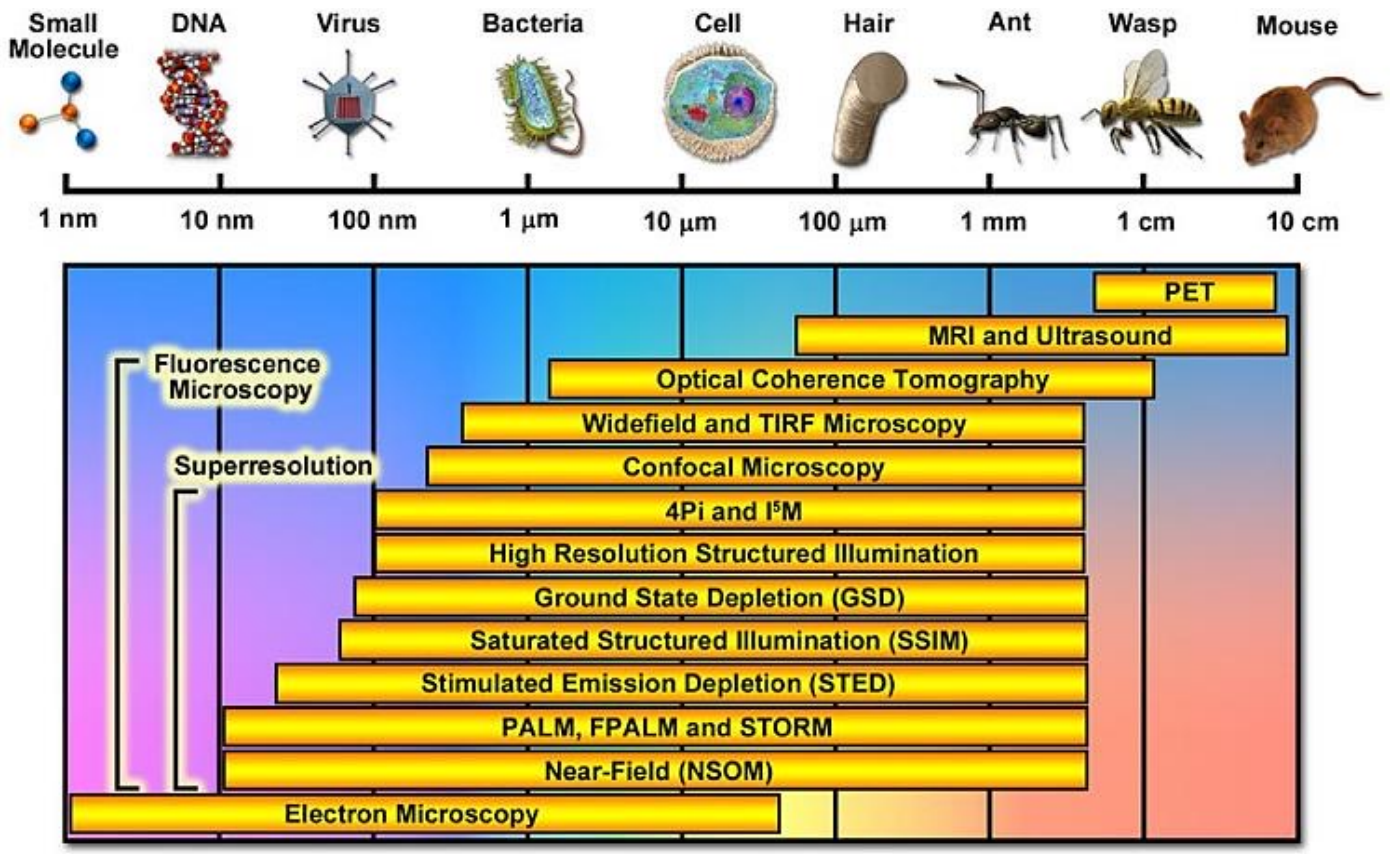

Spatial Resolution and targeting

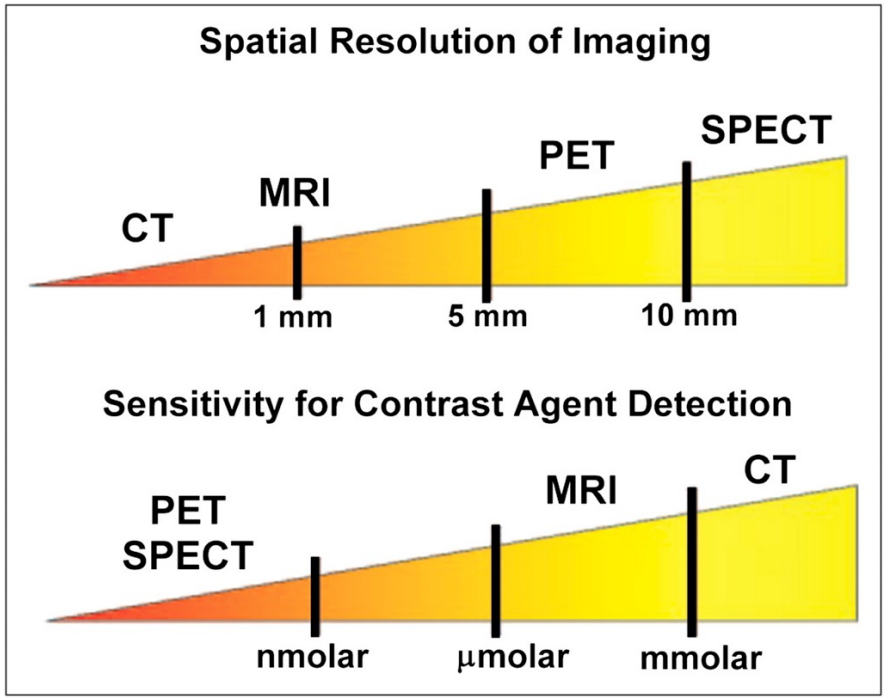

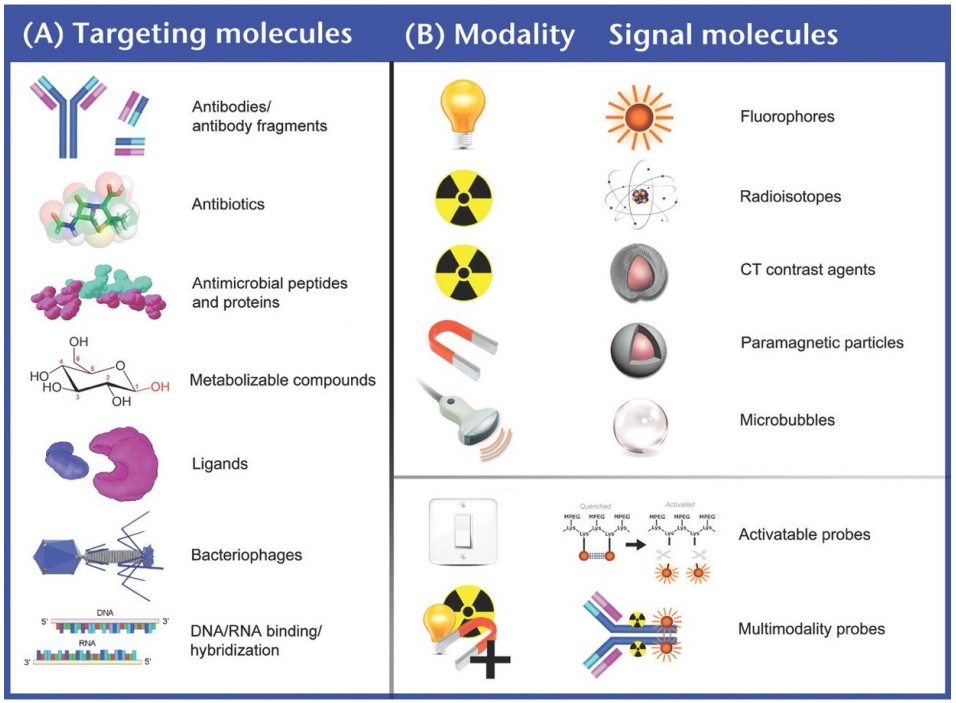

Sadeghi et al. *J Nucl Med* 2010

Memorial Sloan Kettering Cancer Center

Optical Detection

1. Genetically encoded sensors
2. Probe-less strategies
3. Chemical strategies

Optical sensors – Genetically encoded

- Encode a sensor that detects some concentration of a metabolite and then read out fluorescence spatially
- Example of NADH binding creating a bridge and in turn optical detection (Tao et al. *Nat Methods* 2017)

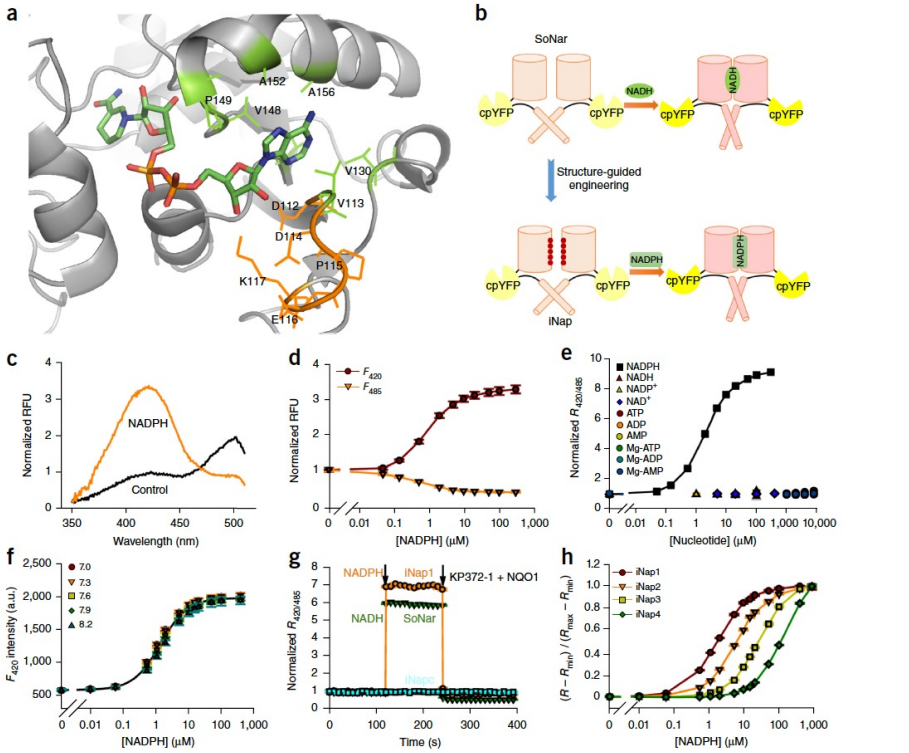

Figure 1 | Structure-guided engineering and characterization of the iNap sensors. (**a**) The NADH binding site of the T-Rex, target for molecular engineering (PDB 1XCB). It contains a charged selective loop (orange) around the 2′-hydroxyl functionality of the ligand and a hydrophobic adenine-binding pocket (green). (**b**) The working mechanism of iNap and SoNar sensors. (**c**) Excitation spectra of purified iNap1 in the control condition (black) and after addition of 100 μM NADPH (orange). Data are normalized to peak intensity at 420 nm in the control condition. Emission was measured at 530 nm. (**d**) iNap1 fluorescence intensity with excitation at 420 nm (F_{420}) or 485 nm (F_{485}) in the presence of different concentrations of NADPH. Emission was measured at 528 nm. (**e**) $R_{420/485}$ of iNap1 in the presence of different concentrations of NADPH or its analogs. (**f**) iNap1 F_{420} intensity (arbitrary units (a.u.)) as a function of NADPH concentration at the indicated pH. (**g**) Kinetics of fluorescence response of purified iNap1 and SoNar protein to 10 μM NADPH and 10 μM NADH, respectively. NADPH or NADH was subsequently decreased (oxidized) by the addition of redox cycling agents containing 1.5 μM KP372-1 and 3 μM NQO1. (**h**) NADPH titration curves of iNap1–iNap4. Binding affinities were determined as 2 μM, 6 μM, 25 μM and 120 μM, respectively. Data in **d**, **e** and **g** are normalized to initial values. In **d**–**h**, experiments were done in triplicate and data are mean ± s.e.m. from 3 independent detections.

Optical sensors – Probe-less strategies

- Detecting autofluorescence, classic experiments from Chance et al. *JBC* 1979
- This has been extended to in cell measurements of NADH and FAD using fluorescence lifetime imaging (Walsh et al. *Cancer Res* 2013)

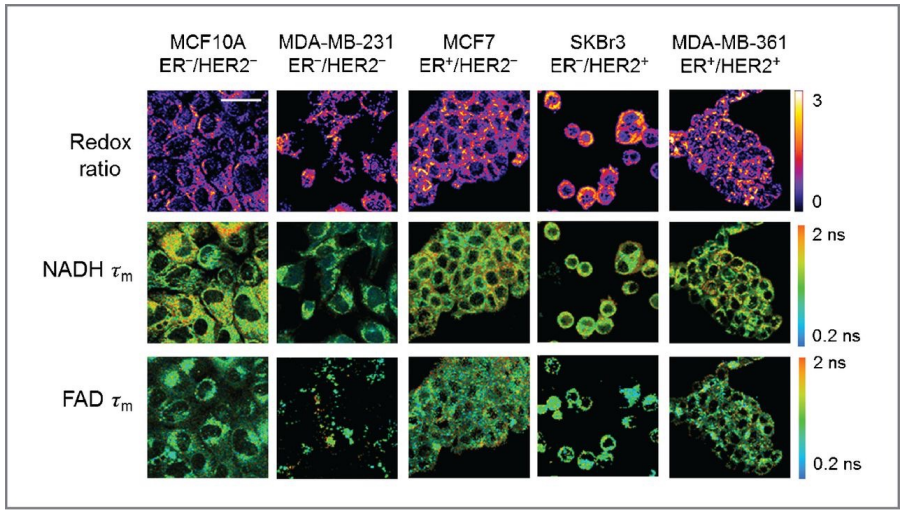

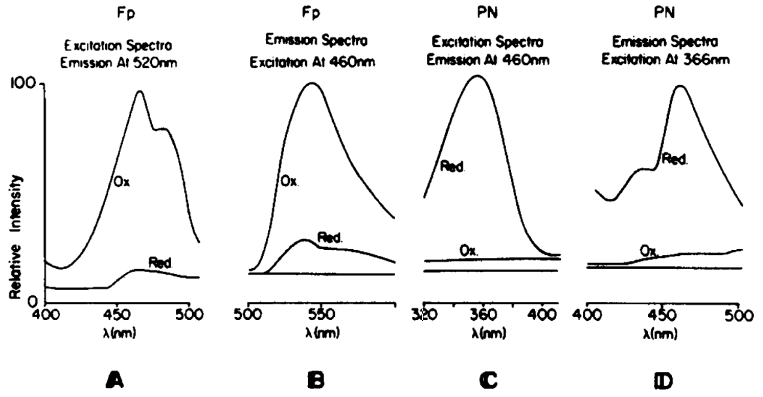

FIG. 3. Excitation and emission spectra of flavoprotein and pyridine nucleotide components of pigeon heart mitochondria at −196°C. *Panel A*, flavoprotein excitation spectrum; *Panel B*, flavoprotein emission; *Panel C*, NADH excitation; *Panel D*, NADH emission at the wavelengths indicated. The oxidized (*Ox.*) and reduced (*Red.*) states were obtained by procedures described under "Methods." The reduced form is the anaerobic State 5. The shoulder on the flavoprotein excitation spectrum at approximately 480 nm is due in part to sharp lines in the xenon arc spectrum of the Hitachi MP-4S spectrophotometer.

Optical sensors – Chemical strategies

- Incubation with a dye (2-NBDG) - Yoshioka et al. *Biochimica et Biophysica Acta* 1996
- Be careful, 2-NBDG isn't glucose!

(Sinclair et al. *Immunometabolism* 2020)

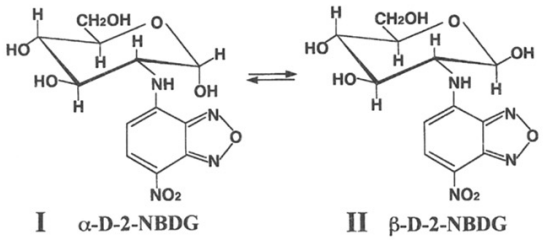

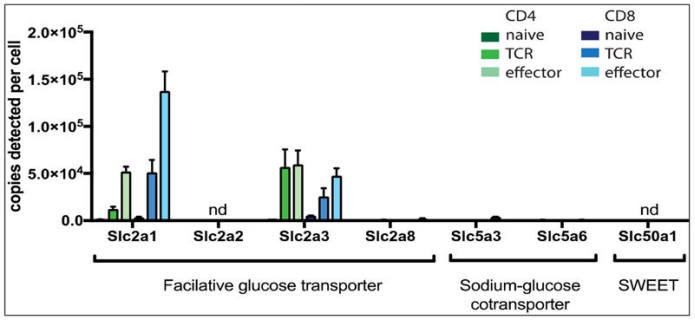

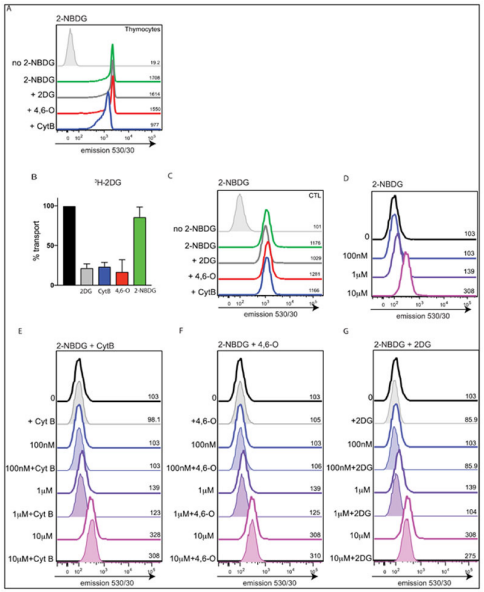

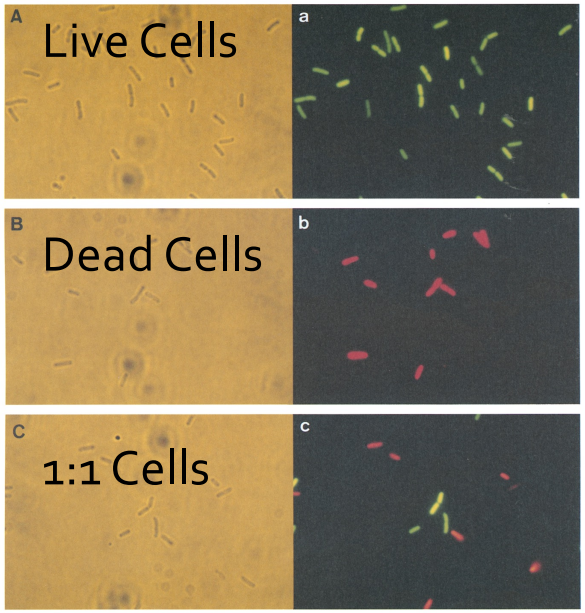

Memorial Sloan Kettering Cancer Center

Electrochemical Detection

- Typically there is a sensor that interacts with the metabolite
  - The sensor helps cells detect fluctuations in metabolite levels.
- This sensor transmits through a transducer
  - Depending on the input (metabolite concentration, nutritional or energy status, etc.), the transducer orders effector proteins to execute the corresponding signal output.
- Ultimately modifying an effector which provides the readout

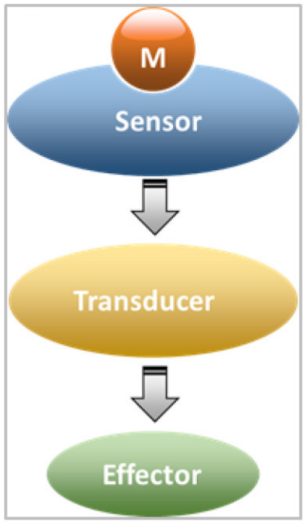

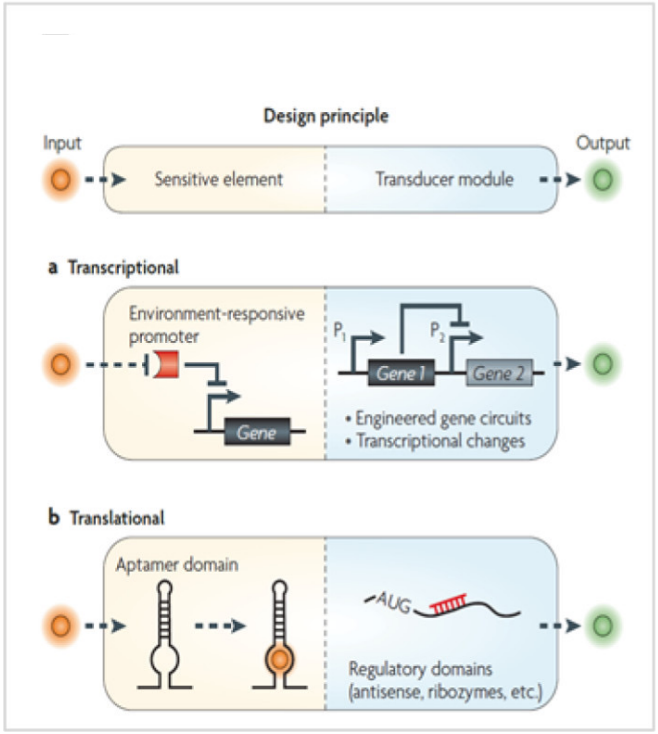

Koklu et al. *Chem Rev* 2022

Electrochemical Detection

- Enzymes are classical recognition mechanisms and can be broken into 6 classes

Enzymes	Reaction type	Description
Oxidoreductases	Redox reaction (electron transfer)	The enzymes can be oxidases or reductases.
	$A_{red} + B_{ox} \leftrightarrow A_{ox} + B_{red}$	Example: glycolysis, oxidative phosphorylation, and amino acid metabolism.
Transferases	Transfer or exchange of an atom or group between substrates	Transferases can be categorized further based on the type of chemical group transferred.
	A–B + C → A + B–C	Example: DNA polymerases and glutathione transferases
Hydrolases	Hydrolysis reactions	The hydrolases are further grouped into 13 subclasses depending on the bonds they act upon, such as cleaving ester bonds, destroying peptide bonds, breaking carbon–nitrogen bonds.
	$A–B + H_2O \rightarrow A–H + B{=}OH$	
Lyases	Nonhydrolytic bond cleavage (bond formation/breaking)	The lyases are classified into 7 subclasses based on the cleaving bonds, including decarboxylases (C–C), oxo acid lyases (C–N), aldehyde lyases (C–O).
	A–B ↔ A + B	
Isomerases	Conversion of isomers, geometric isomers, or optical isomers	The isomerases are assigned into 6 subclasses based on the involved molecules such as *cis–trans* isomerases, intramolecular oxidoreductases.
	A–B–C ↔ A–C–B	
Ligases	Catalyze the synthesis of two molecular substrates into one molecular compound	Ligases use ATP as a cosubstrate and are categorized into 6 subclasses depending on the formation of new chemical bonds such as C–O, C–S, C–N.
	$A + B + ATP \rightarrow A–B + ADP + P_i$	

Electrochemical Detection

Table 2. Comparison of Recognition Units for Metabolite Sensors

	Enzymes	Antibodies	Aptamers	Riboswitches	MIPs
Stability	Temperature-sensitive	Easily denatured	Withstand repeated rounds of denaturation−renaturation	Highly sensitive to the environmental conditions	Chemically stable Physically Stable Excellent reusability
	pH-sensitive	Temperature-sensitive	Stable at room temperature		Shelf life of several years at room temperature
	Limited shelf life	Limited shelf life	Long shelf life (several years)		
	Can be lyophilized	Must be refrigerated for storage and transport	Can be lyophilized		
	Must be refrigerated once in the solution for storage				
Synthesis	Produced from micro-organism	Produced *in vivo* (+6 months)	*In vitro* (2−8 weeks)	Produced from both prokaryotic and complex organism in a high throughput manner	Two-step process: polymerization followed by template removal
	Often needs purification	Batch-to-batch variations	No batch-to-batch variation	Quick synthesis	Low cost
	Variability in batch-to-batch activity (“activity range”)	Laborious and expensive			
Modifiability	Modifiable without affinity loss	Modifications often lead to reduced activity	Readily and easily be modified without affinity loss	Readily tuned by mutating the sequences	Tunability
	Mutation			Highly versatile	
Affinity/ Sensitivity	High sensitivity	Dependent on the number of epitopes on the antigen	High and increased in multivalent aptamers	High sensitivity	Highly dependent on the template/ monomer interactions
	pH sensitivity	pH sensitivity		Environmental (genetics) sensitivity	
		Disrupted by high salt concentrations			
Specificity	The same enzyme can catalyze different substrates	Different antibodies might bind the same antigen	Single point mutations identifiable	High specificity	Versatile, scalable alternative to natural recognition unit
Cost	Expensive	Monoclonal vs Polyclonal Expensive	Cheap to synthesize	Cheap	Cheap

Positron Emission Tomography (PET)

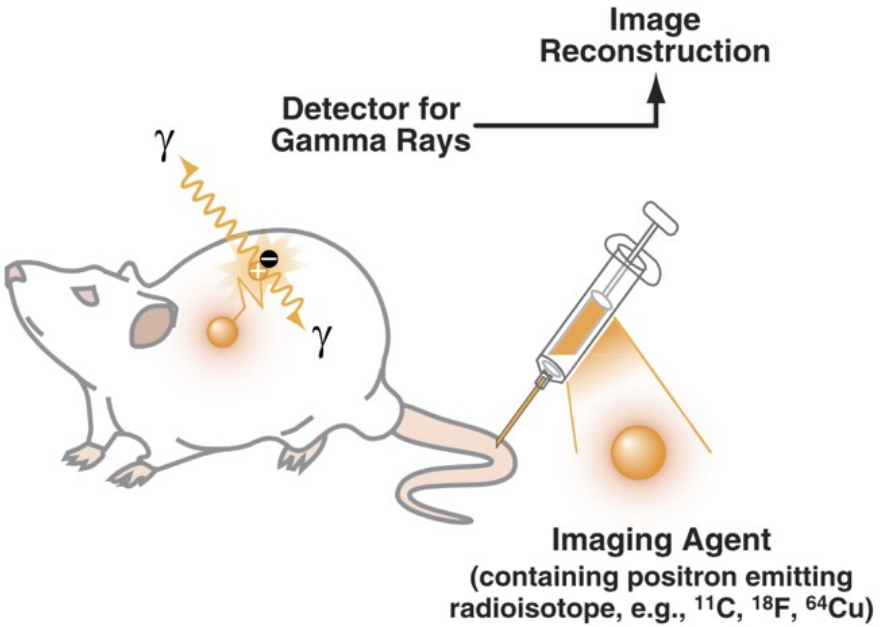

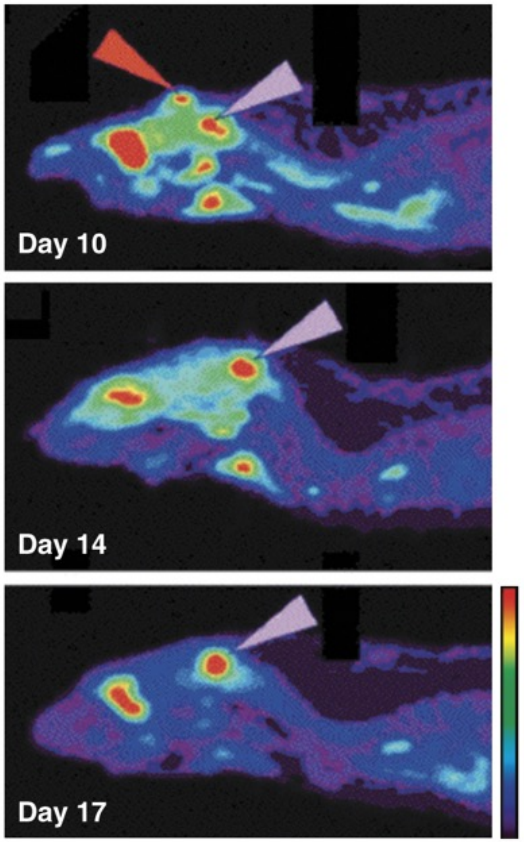

Key Strengths

- Limitless depth of penetration
- Excellent sensitivity
- Quantitative data
- Clinical utility

Key Limitations

- Relatively expensive
- Requires cyclotron/generator
- Ionizing radiation
- Limited spatial resolution
- No multiplexing

James and Gambhir *Physiological Rev* 2012

Memorial Sloan Kettering Cancer Center

Radioisotopes for PET

Isotope	*Half-life*	β^+ *Energy (MeV)*	γ *Energy (MeV)*
C-11	20.4 m	0.385 (99.8%)	
N-13	9.97 m	0.492 (99.8%)	
O-15	122 s	0.735 (99.9%)	
F-18	110 m	0.250 (100%)	
K-38	7.64 m	1.216 (99.3%)	2.167 (99.8%)
Cu-62	9.74 m	1.315 (97.6%)	
Cu-64	12.7 h	0.278 (17.9%)	
Ga-68	68.1 h	0.836 (8.79%), 0.352 (1.12%)	1.077 (3.0%)
Rb-82	75 s	1.523 (83.3%), 1.157 (10.2%)	0.776 (13.4%)
I-124	4.18 d	0.686 (11.3%), 0.974 (11.3%)	1.691 (10.4%), 7.228(10.0%), 1.509 (3.0%), 1.376 (1.7%), 1.325 (1.43%)

The average energy of the β^+ is given along with the percentage of decays in which the β^+ is emitted. The energy of gamma rays that occur in more than 1% of decays is given along with the percentage of decays in which that gamma ray is emitted.

Jadvar and Parker *Clinical PET and PET/CT* 2005

Radiosynthesis of ^{11}C compounds ($T_{½}$ = 20.4 min)

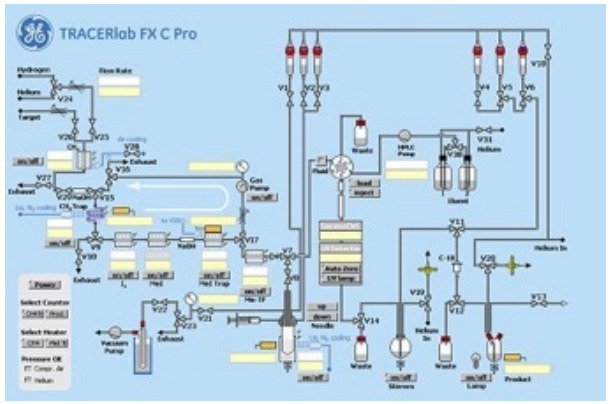

1975 - ^{11}C-glucose was prepared by photosynthesis using Swiss chard leaves. Mashed up, extracted and a "green solution" injected into humans

2012 - ^{11}C-glucose is prepared by a "black box" automated versatile synthesizer producing drugs ready for human use

Memorial Sloan Kettering Cancer Center

Glucose Uptake ^{18}F-FDG

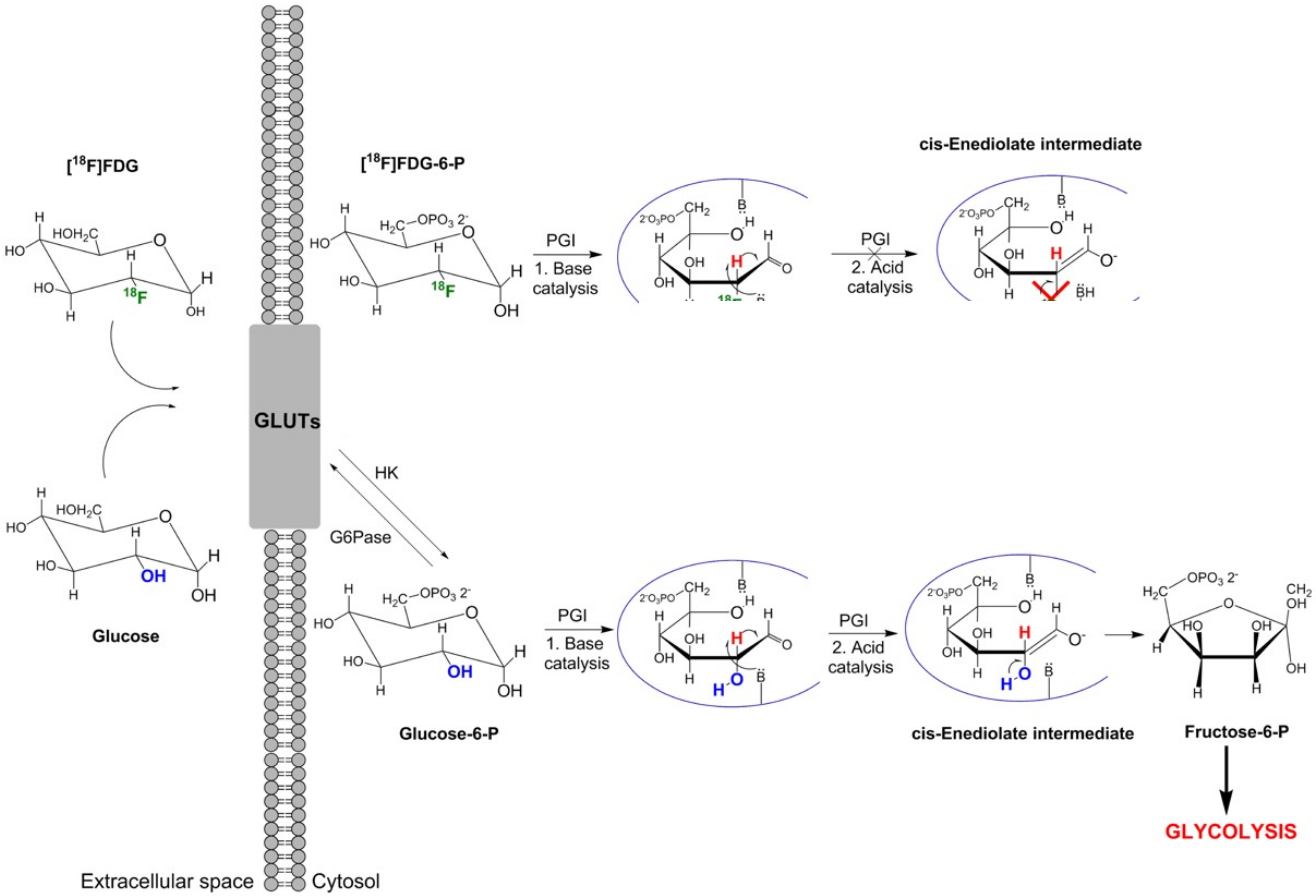

Di Gialleonardo et al *Seminars in Nuc Med* 2016

Memorial Sloan Kettering Cancer Center

Glucose Uptake ^{18}F-FDG v. ^{18}F-FGln

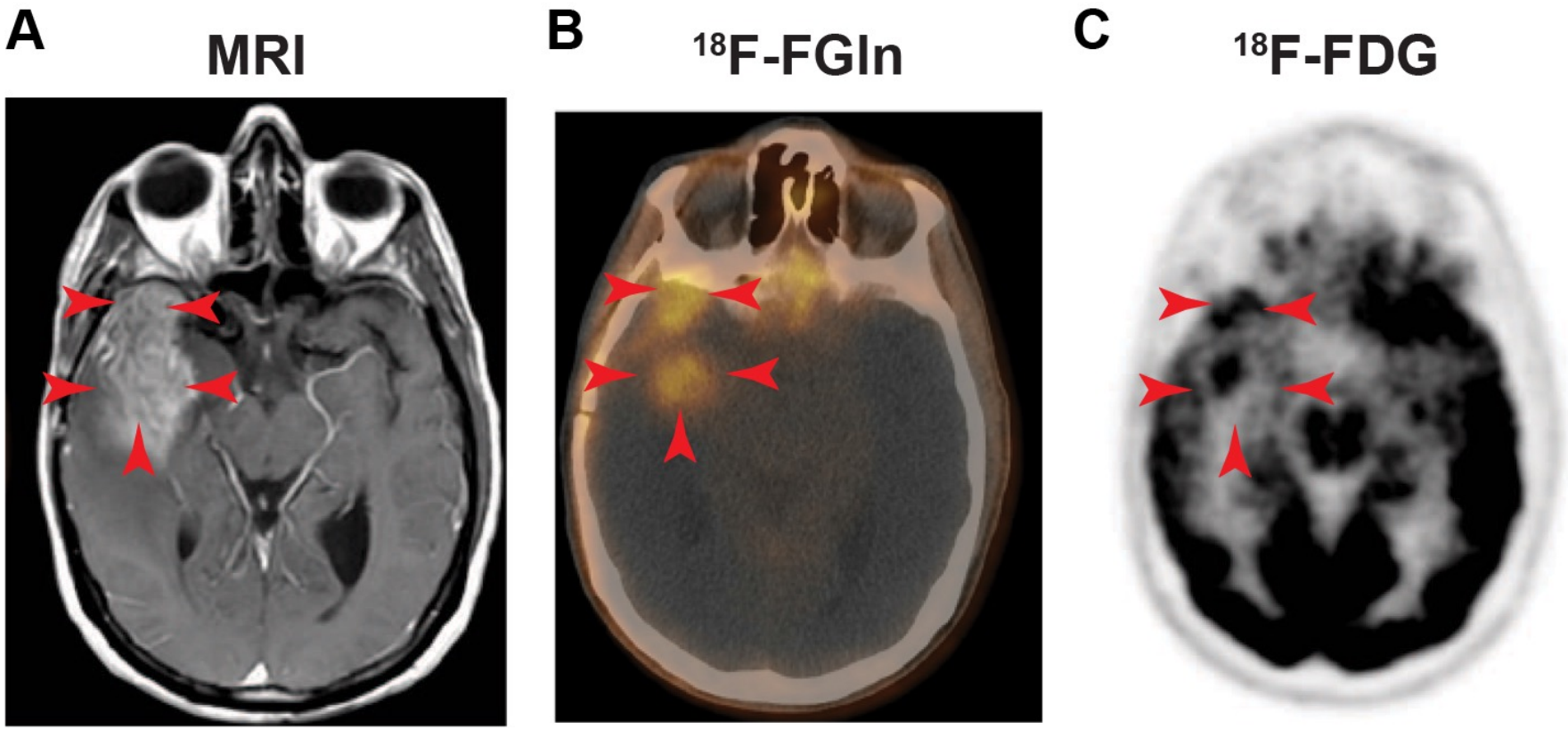

Venneti et al *Science Trans Med* 2015

Memorial Sloan Kettering Cancer Center

Fatty Acid Uptake - ^{11}C-acetate

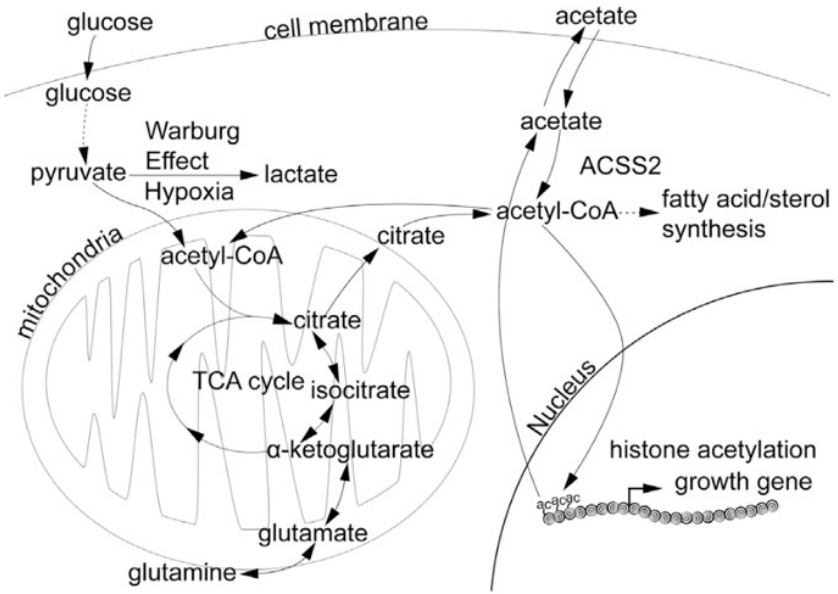

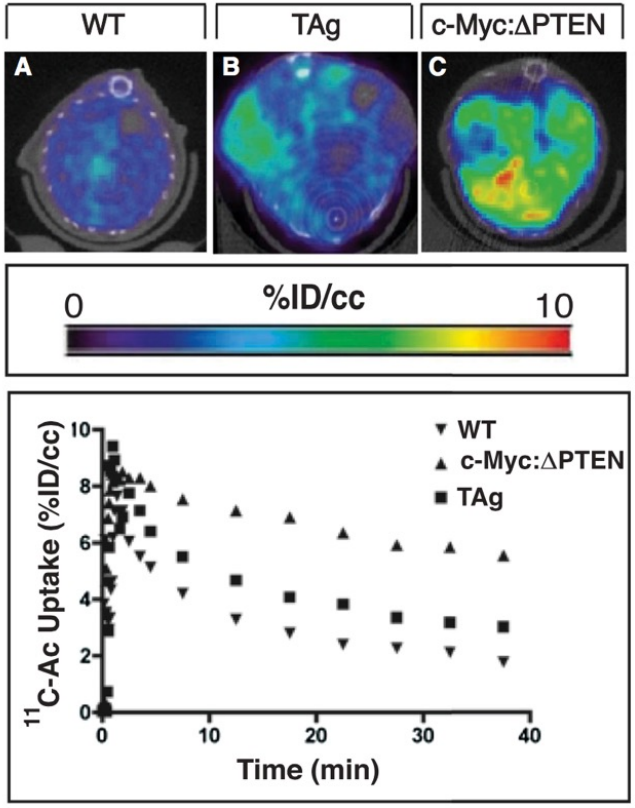

- TAg = develop specific liver cancer, doxycycline (dox)-regulated transgene encoding the SV40 early region (ApoE-rtTAM2:TRE2-TAg)
- C-Myc overexpression and PTEN loss

Comerford et al *Cell* 2014

Memorial Sloan Kettering Cancer Center

Hypoxia – ^{18}FMISO

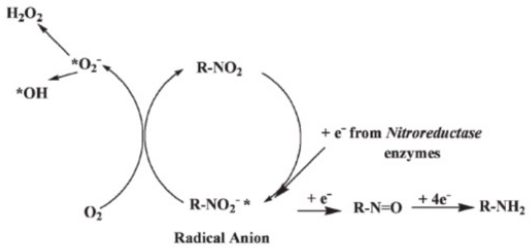

Fig. 15.27 The mechanism of intracellular trapping of nitroimidazoles. Under hypoxic conditions, the nitro group undergoes electron reduction to form reactive radicals which after further reduction form covalent bonds with intracellular macromolecules

[^{18}F]Fluoromisonidazole (FMISO)

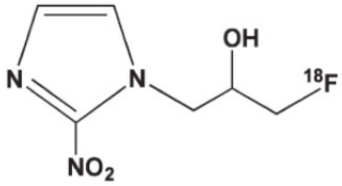

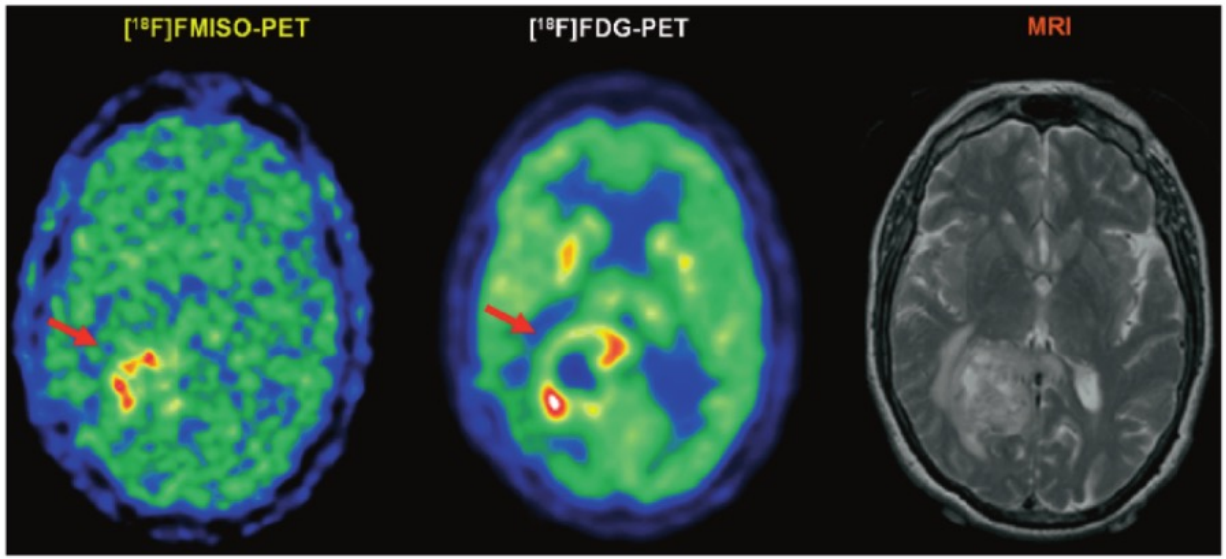

Rasey et al *Radiat Res* 1987

Memorial Sloan Kettering Cancer Center

A thought experiment

- Could you combine positional labeling with radioactivity to resolve pathway flux?

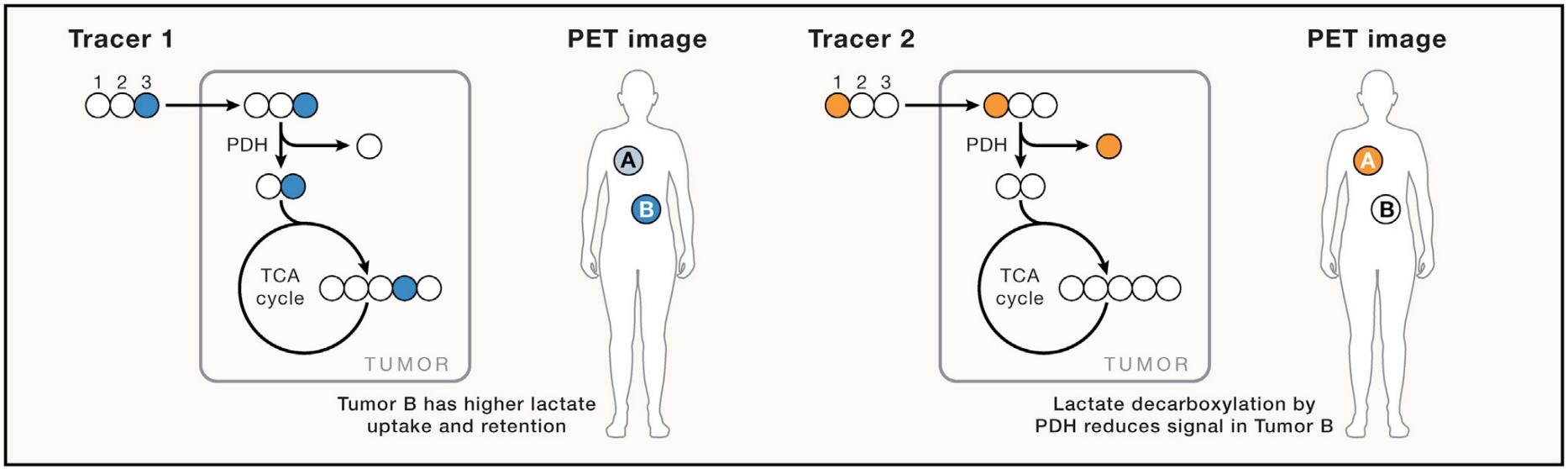

Magnetic Resonance Imaging (MRI)

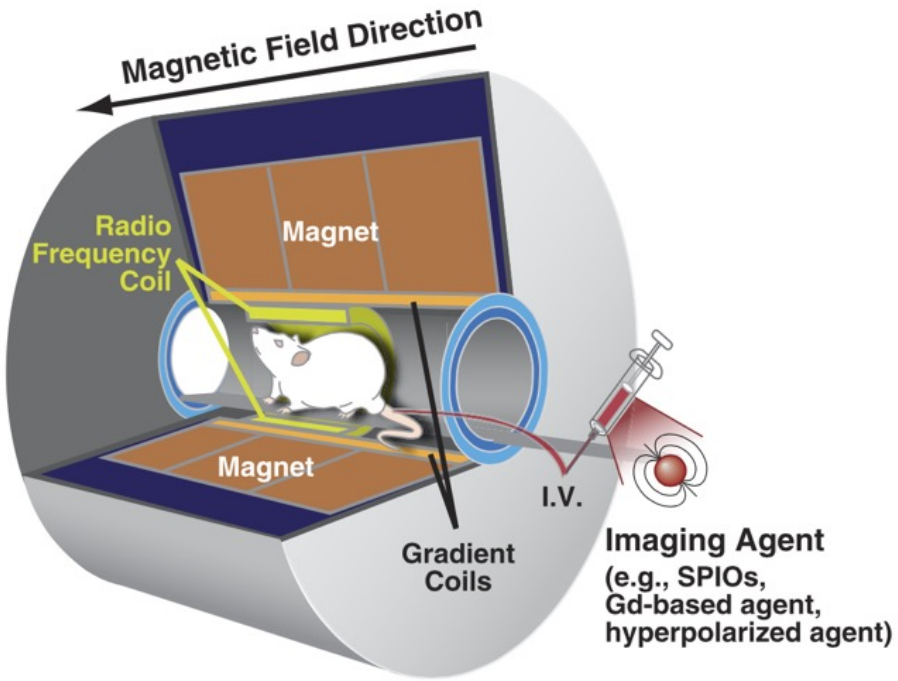

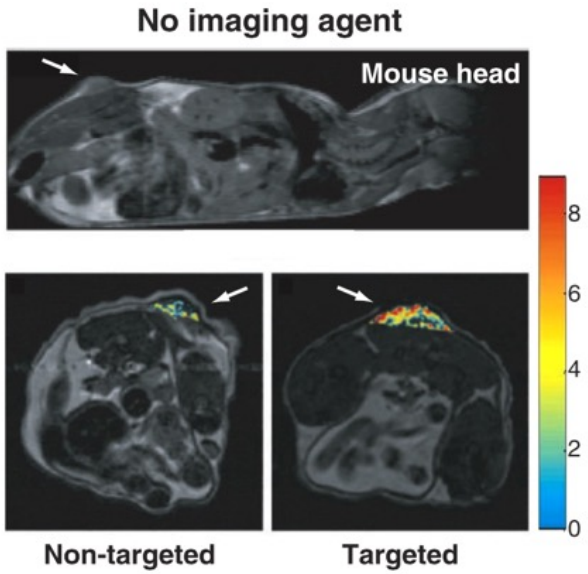

Key Strengths

- Limitless depth of penetration
- High spatial resolution
- Quantitative data
- No ionizing radiation
- Clinical utility

Key Limitations

- Poor sensitivity (requires large mass of imaging agent)
- Relatively expensive
- Relatively poor temporal resolution

James and Gambhir *Physiological Rev* 2012

Memorial Sloan Kettering Cancer Center

NMR/MRI active isotopes

Nuclei	*m* (spin)	Natural abundance (%)	γ (rel to ^{1}H)	$\Delta\delta$ (ppm)	T_1 range	Example biomedical application
^{1}H	1/2	99.98	1	13	0.1–2 s	Total body MRI and MRSI
^{2}H	1	0.02	0.1535	13	<1 s	Metabolic tracer injection using MRSI
^{13}C	1/2	1.11	0.2515	200	0.1–100 s	Metabolic tracer injection using MRSI
^{15}N	1/2	0.37	0.1013	900	0.1–400 s	Metabolic tracer injection using MRSI
^{17}O	5/2	0.04	0.1355	1160	5–50 ms	Oxidative metabolism using MRSI
^{19}F	1/2	100.00	0.9409	700	0.1–1 s	Tracer injection of therapies using MRSI
^{23}Na	3/2	100.00	0.2645	72	10–50 ms	Neurodegeneration and cardiac using MRI
^{31}P	1/2	100.00	0.4048	430	0.05–2 s	Bioenergetics and pH using MRSI

MRI – magnetic resonance imaging, MRSI – magnetic resonance spectroscopic imaging, *m* – quantum spin number, γ – gyromagnetic ratio, $\Delta\delta$ – chemical shift.

We can now get really high-resolution images of structures in the body

not really something you want someone to biopsy…

With high resolution, maybe there is a chance to infer interesting biology

e.g. reduced contrast enhancement = hypoxia

But it is still an inference, not a direct measurement

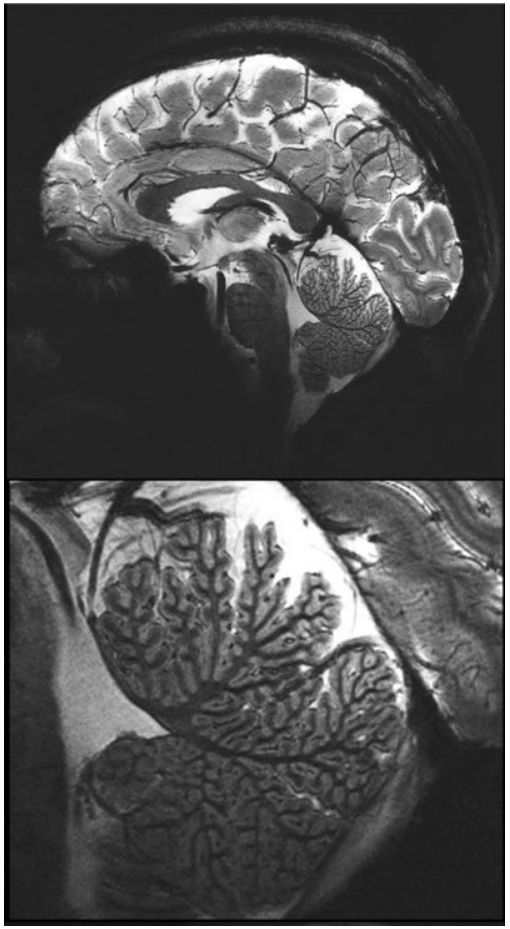

11.7T MRI

Memorial Sloan Kettering Cancer Center

Boulant et al. *Nat Methods* 2024

MR Spectroscopic Imaging (MRSI)

- What about detecting metabolites as opposed to structure?
  - MRI - mainly water 55 M, MRSI – metabolites ~5mM
    → Signal ~ 10,000x smaller!
  - End up w/ lower spatial resolution, longer scans but adds a new dimension

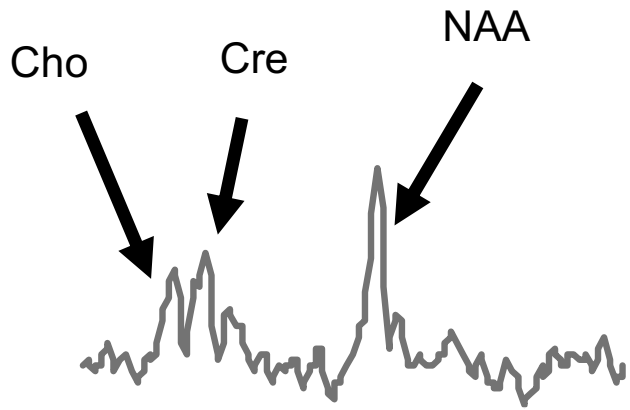

Healthy Brain

Steady state pool sizes ^{1}H MRSI

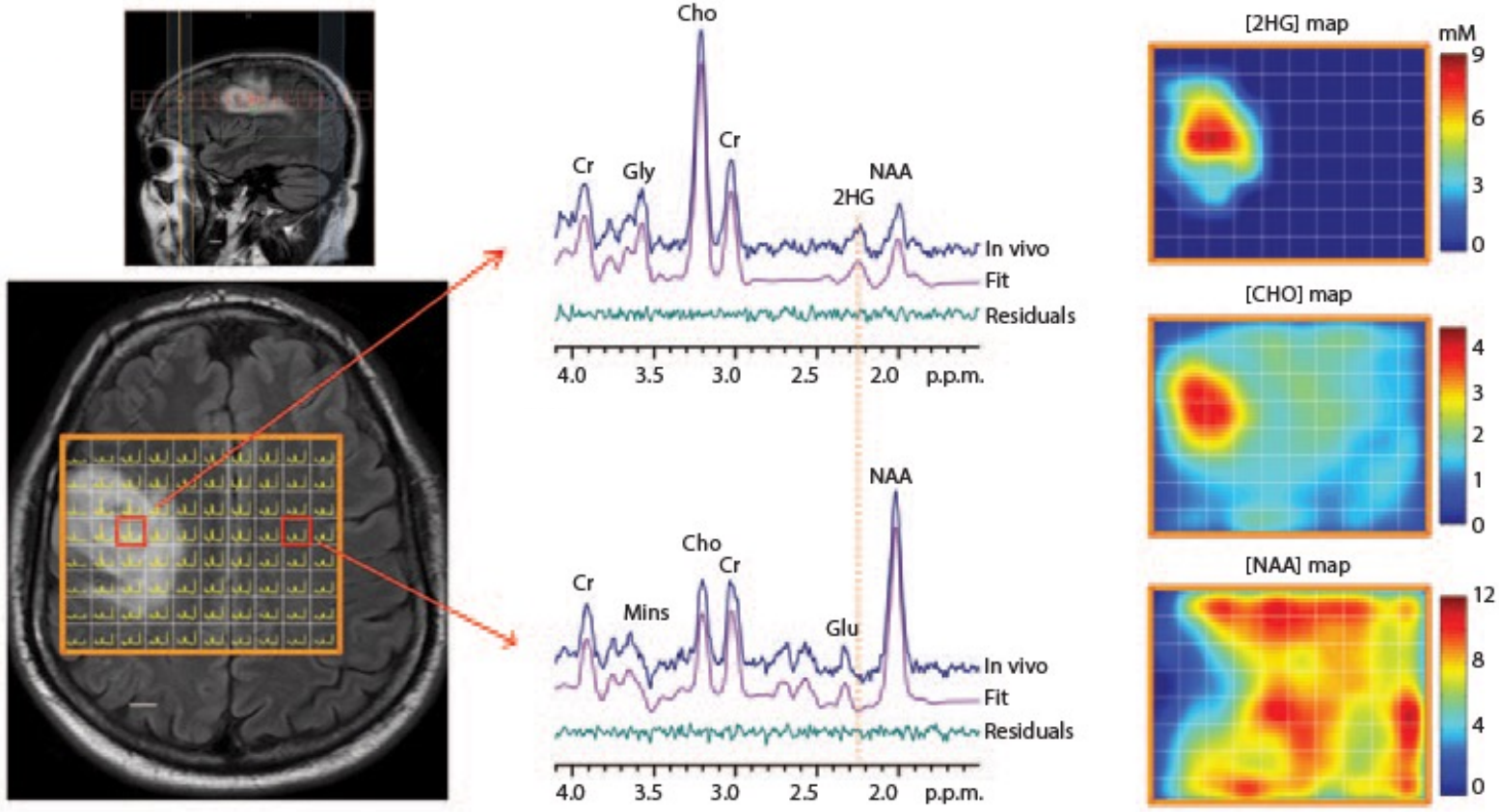

Choi et al *Nature Med* 2012

Memorial Sloan Kettering Cancer Center

Ultra-fast J-resolved MRSI pushes the resolution to reveal small foci of metabolic changes

Brain tumors

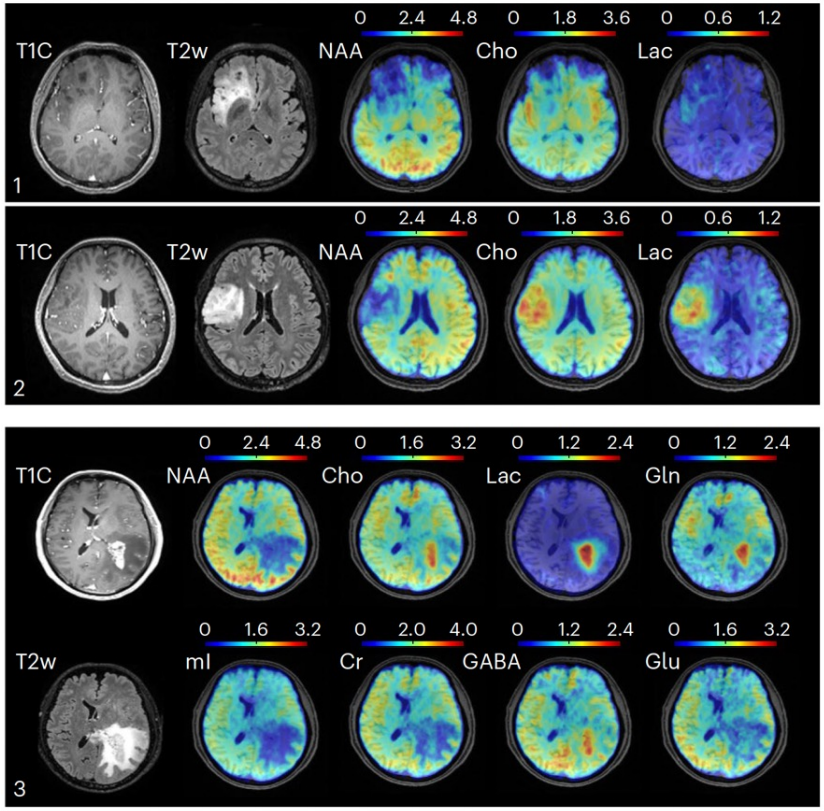

Zhao et al *Nat Biomed Eng* 2025

MS lesions

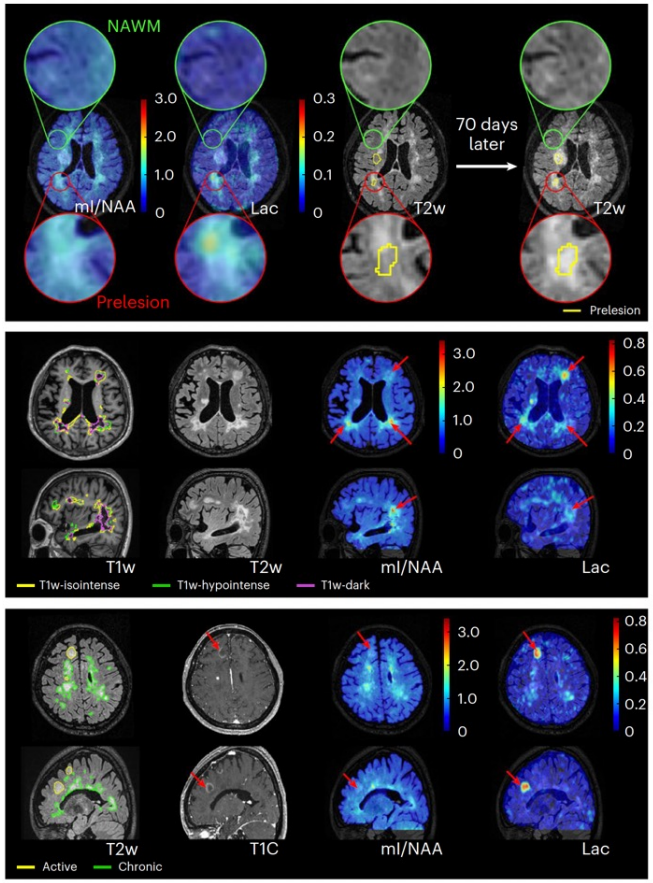

Bioenergetics – ^{31}P MR Spectroscopy

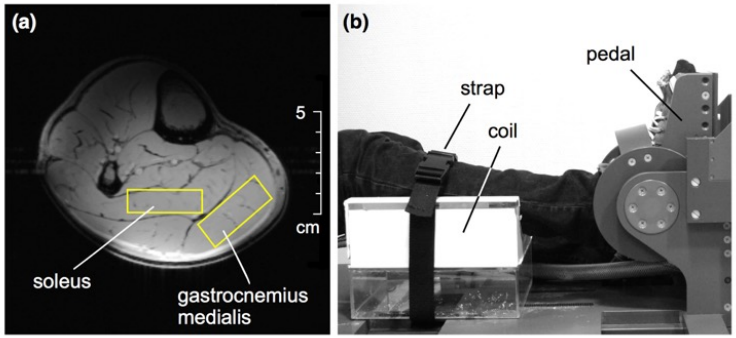

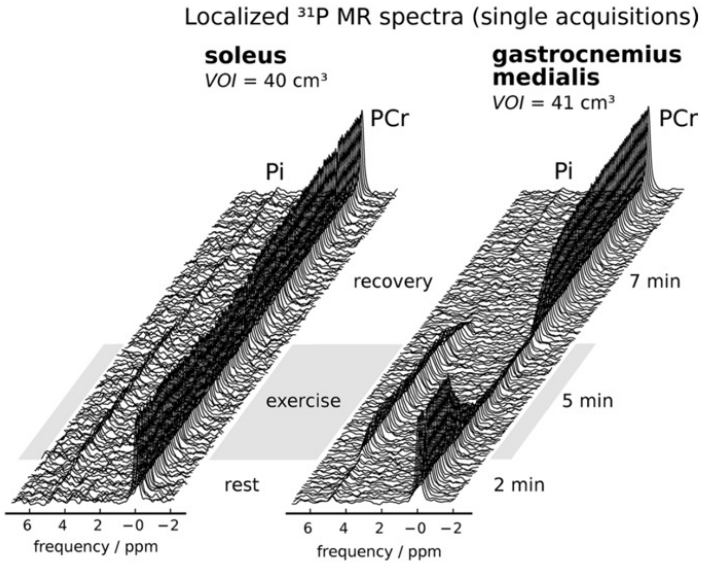

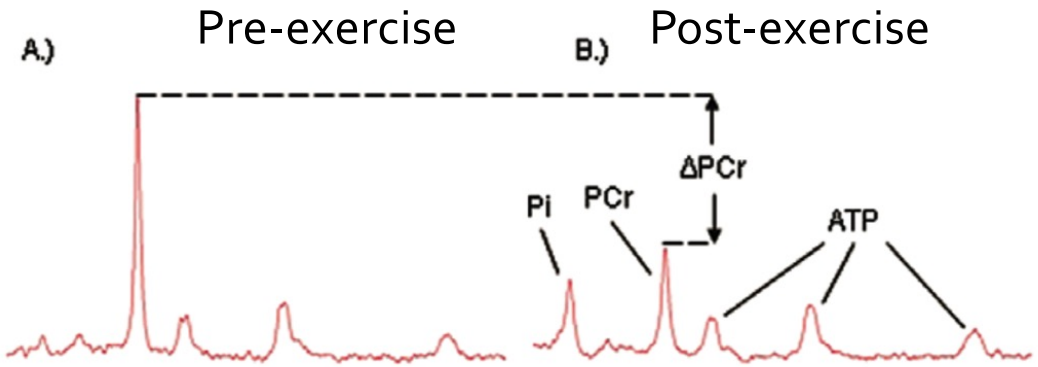

Fiedler et al 2015

Memorial Sloan Kettering Cancer Center

^{13}C-acetate MR Spectroscopy to measure real time flux in the liver

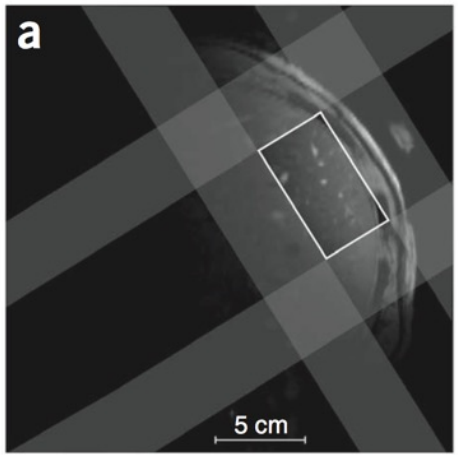

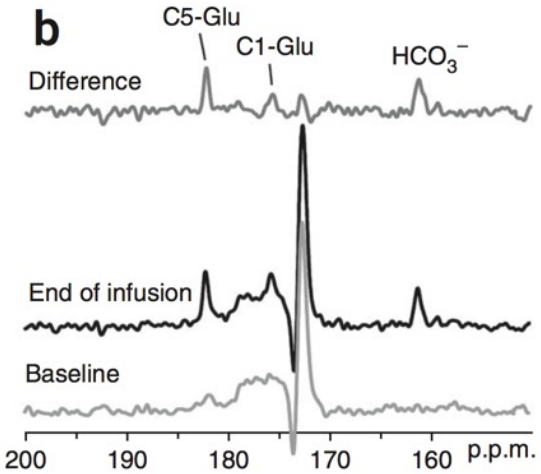

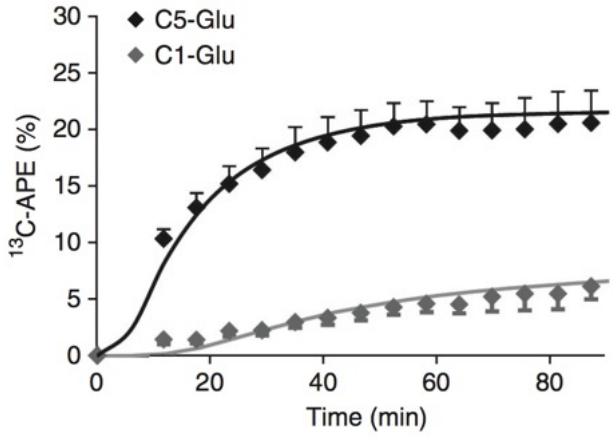

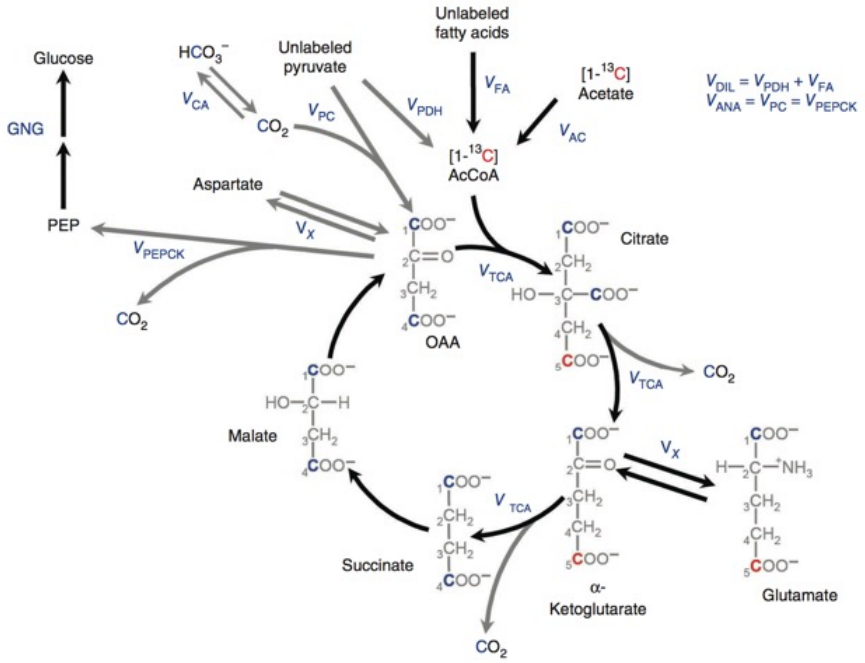

Befroy et al *Nat Med* 2014

Memorial Sloan Kettering Cancer Center

Hyperpolarized ^{13}C Magnetic Resonance

- HP MRI provides a mechanism to overcome the sensitivity problem of MR by aligning spins outside of the magnet
- Follow the conversion of HP pyruvate through many pathways in seconds!
  - Reduction to HP Lactate
  - Transamination to HP Alanine
  - Decarboxylation to HP carbon dioxide and later bicarbonate (pH)

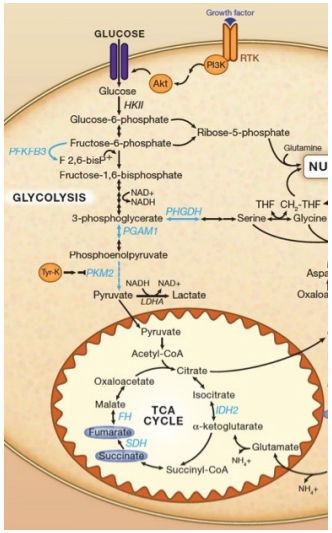

Keshari and Wilson *Chem Soc Rev* 2014

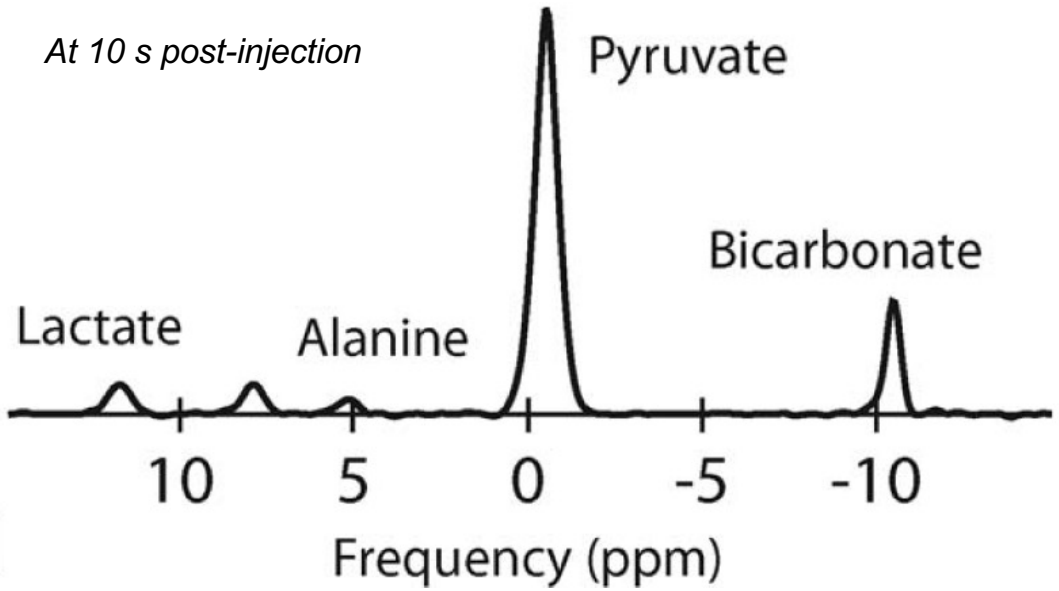

orial Sloan Kettering
er Center

HP MRI in humans facilitates imaging isotope tracing

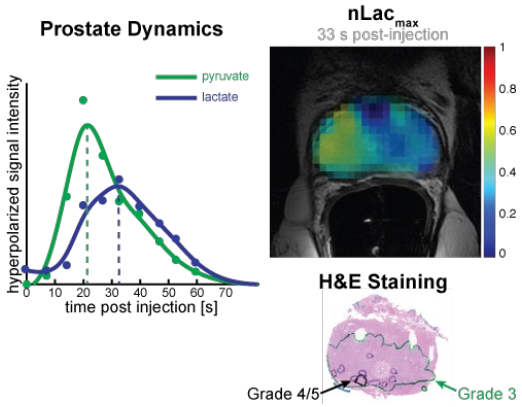

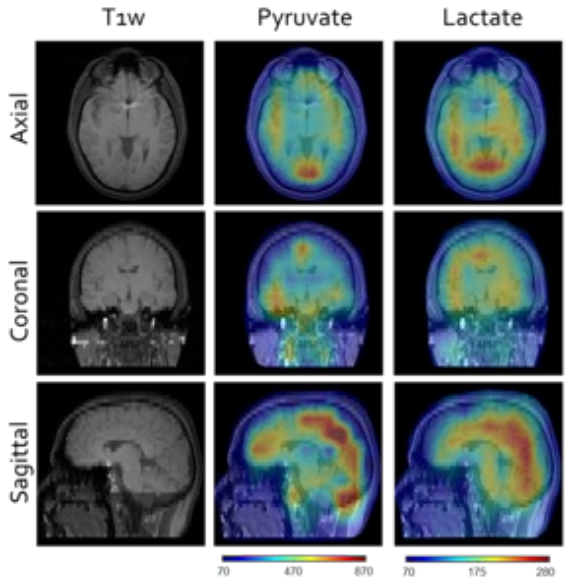

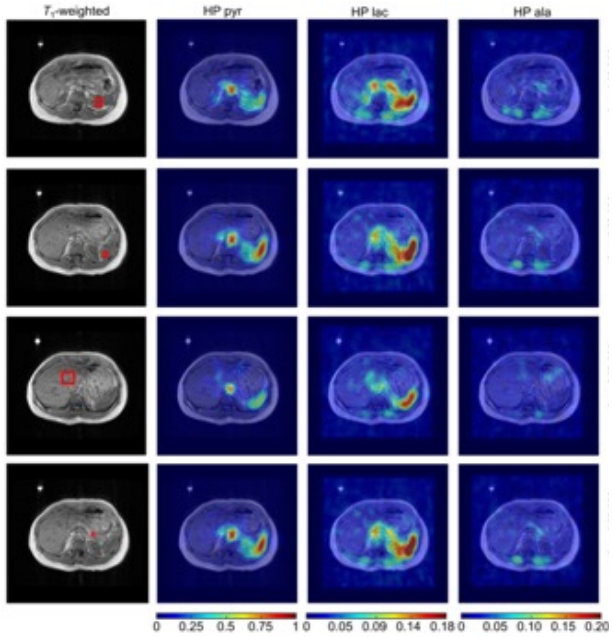

Miloushev et al. *Cancer Res* 2018
Granlund et al. *Cell Metabolism* 2020
Deh et al. *MRM* 2024
Zhang et al. *JMRI* 2024

Memorial Sloan Kettering Cancer Center

Back to the Pool v. Flux

- Each detection method can provide weighting to the steady state pool, the flux or both
- Sometimes the answer can be inferred from the steady state pool
- Most often flux is more sensitive to changes than the pool size

VS

Engineering Metabolism

Can we manipulate the metabolism of a cell to do what we want?

What can we learn from model organisms?

Success stories of Metabolic Engineering

Table 1. Some Success Stories of Metabolic Engineering

Chemical	Application	Cell Factory	Companies
Lysine	feed additive (>1 million tons/year)	*Corynebacterium glutamicum*	Evonik, ADM, CJ, Ajinomoto
1,3-Propanediol	chemical building block, e.g., for production of materials, cosmetics, and food ingredients	*Escherichia coli*	Dupont and Tate&Lyle joint venture
7-ADCA	precursor for the broad-spectrum antibiotic Cephalexin	*Penicillium chrysogenum*	DSM
1,4-Butanediol	chemical building block, e.g., for production of Spandex	*Escherichia coli*	Genomatica
Artemisinic acid	anti-malarial drug	*Saccharomyces cerevisiae*	Sanofi Aventis (process developed by Amyris)
Isobutanol	advanced biofuel	*Saccharomyces cerevisiae*	Gevo, Butamax

Nielsen and Keasling *Cell* 2016

Design principles of metabolic engineering

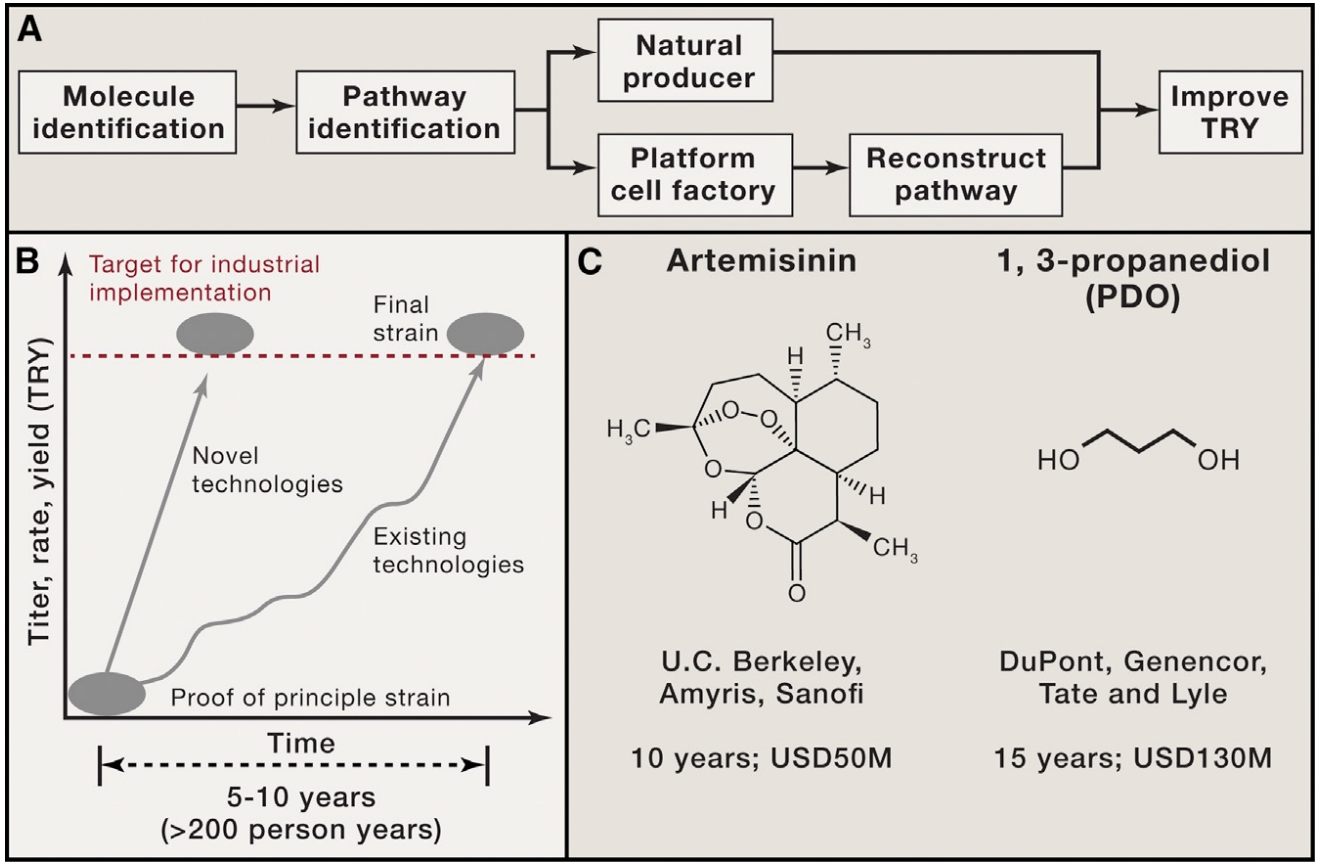

Re-routing metabolism

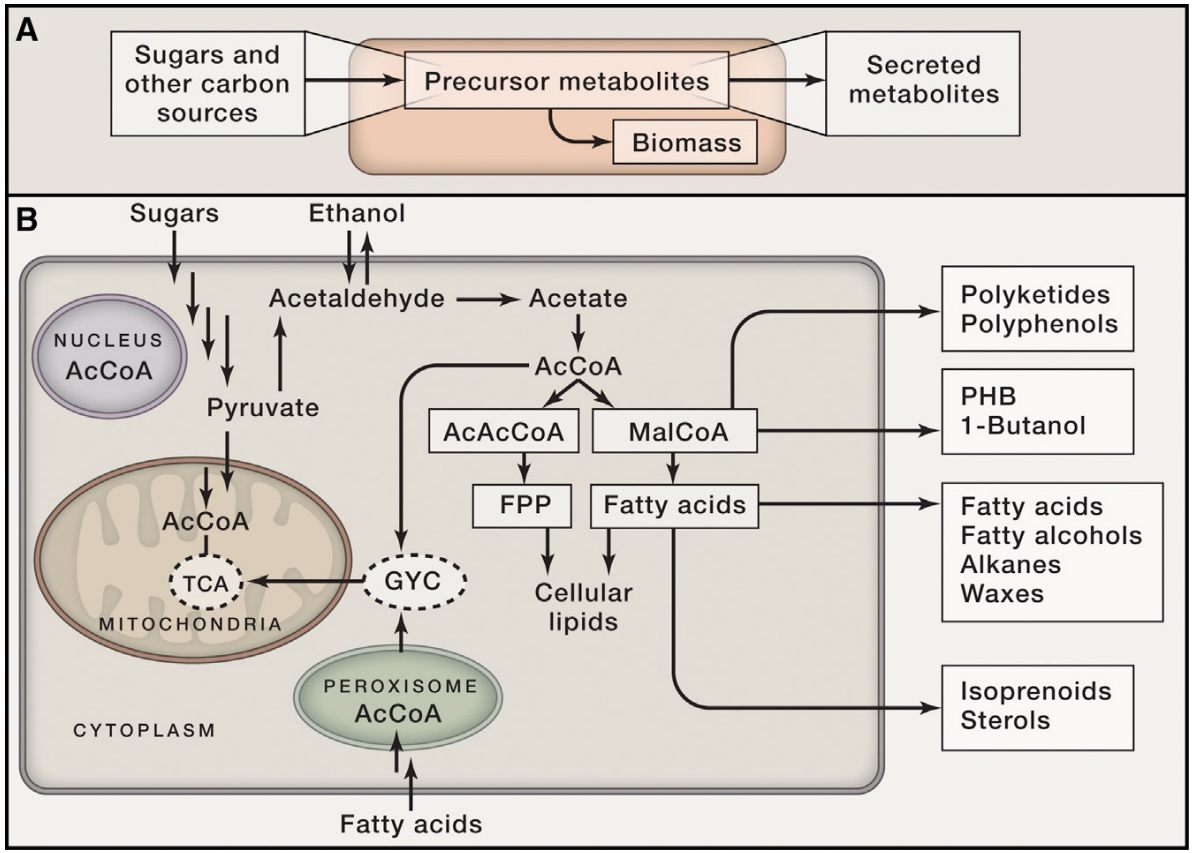

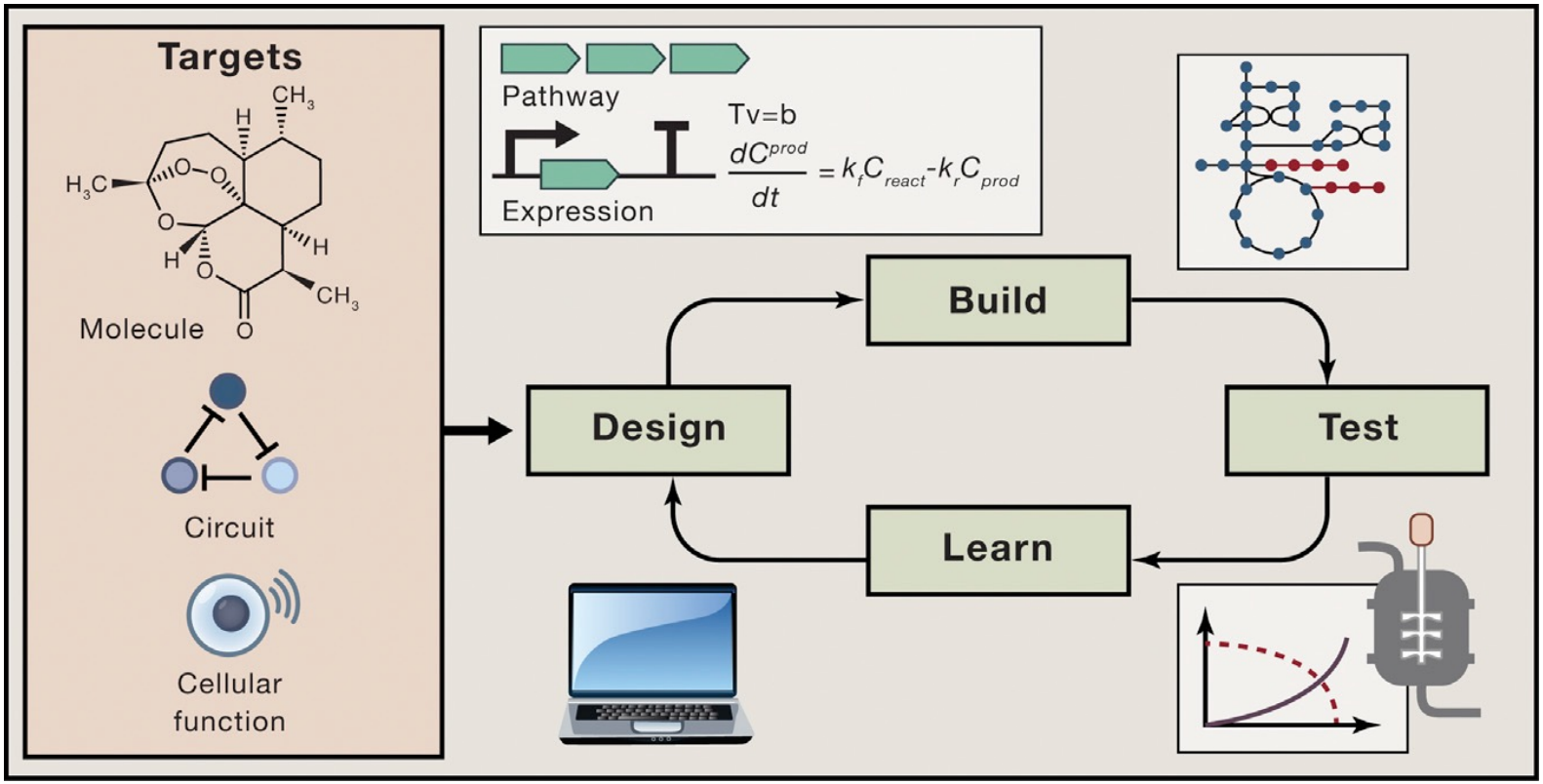

Memorial Sloan Kettering Cancer Center

What if we took all that modeling and tried to make a human model?

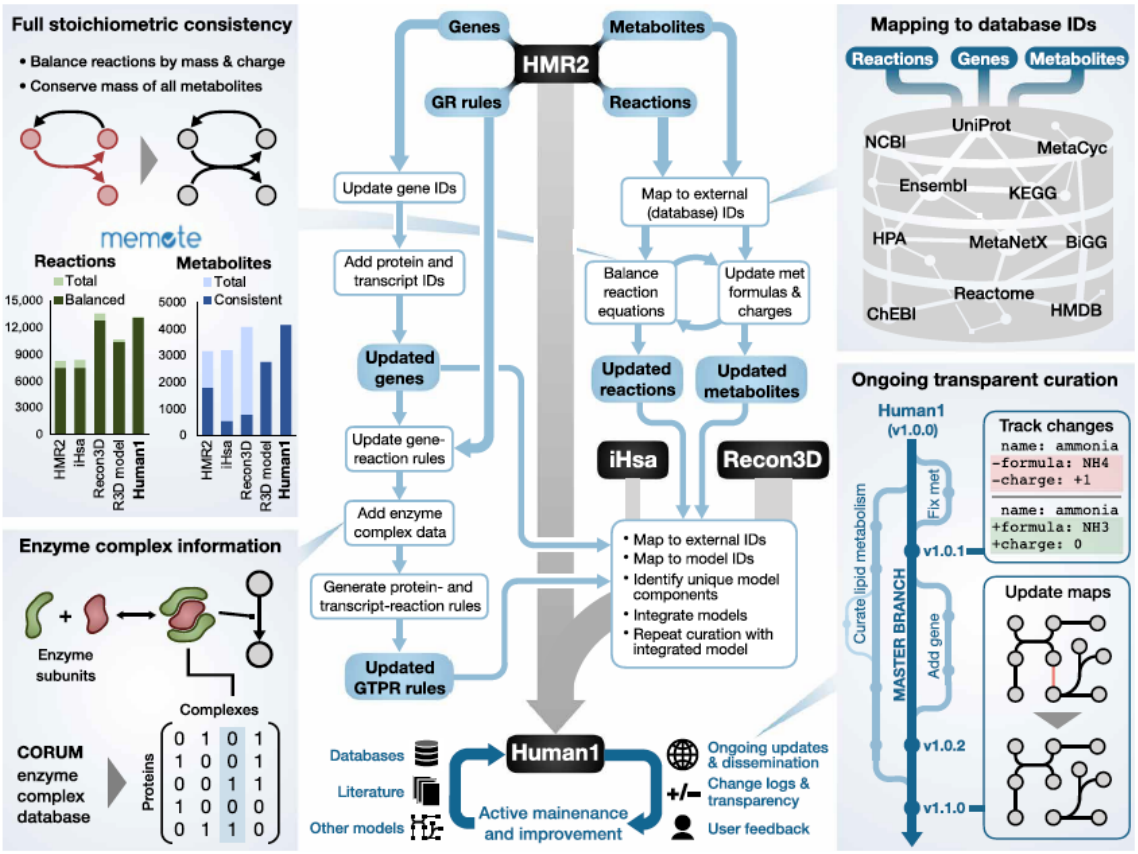

Robinson *Sci Signaling* 2020

Memorial Sloan Kettering Cancer Center

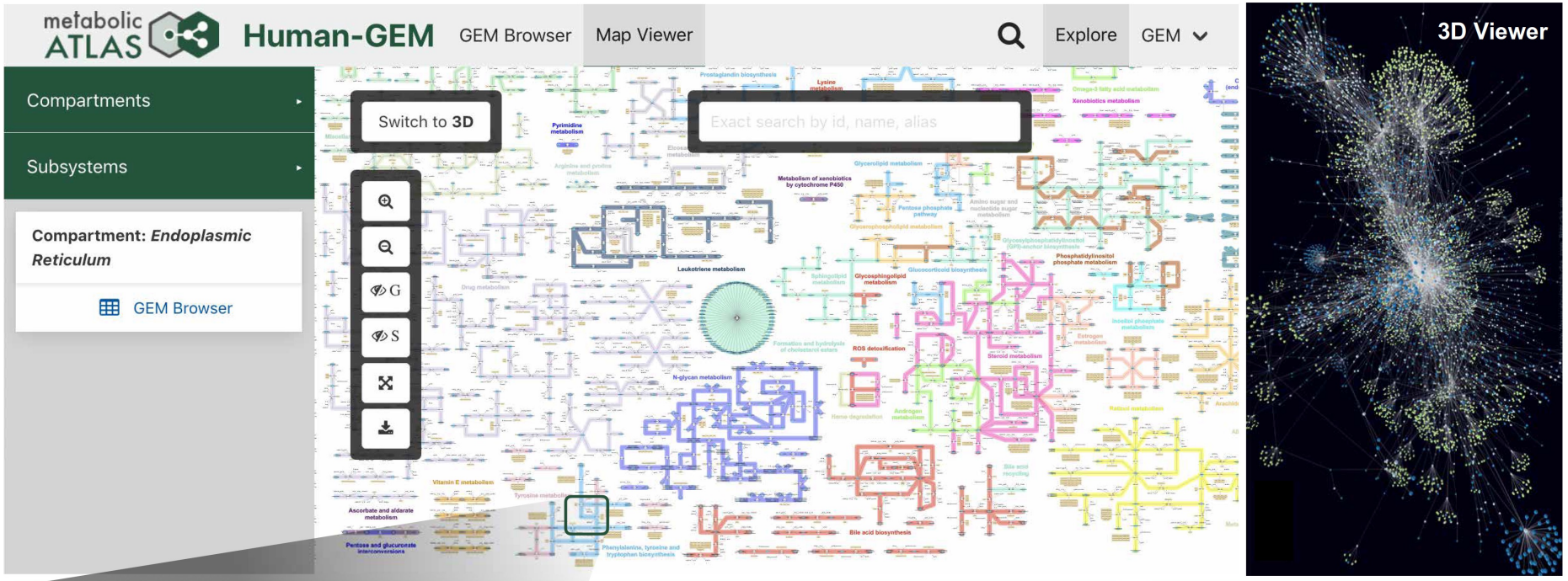

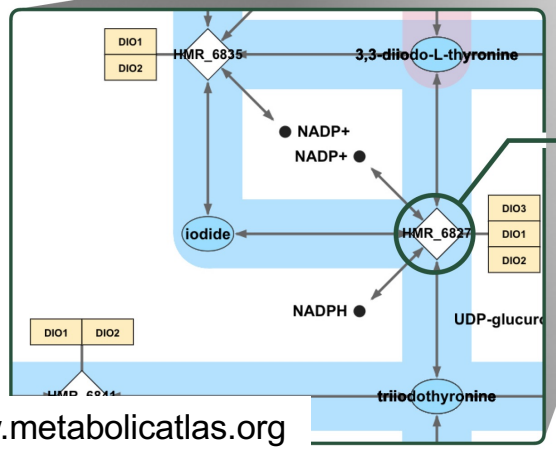

GEM Browser

Human-GEM ID	HMR_6827
Equation	3,3-diiodo-L-thyronine + iodide + NADP+ ⇔ NADPH + triiodothyronine
Reversible	Yes
Quantitative	Lower bound: -1000 - Upper bound: 1000
Gene rule	DIO3 or DIO2 or DIO1
EC	EC:1.97.1.10 EC:1.97.1.11
Compartment(s)	Endoplasmic reticulum
Subsystem(s)	Phenylalanine, tyrosine and tryptophan biosynthesis

DIO2 Interaction Partners

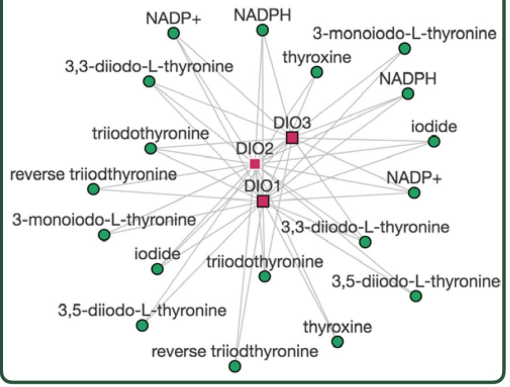

www.metabolicatlas.org

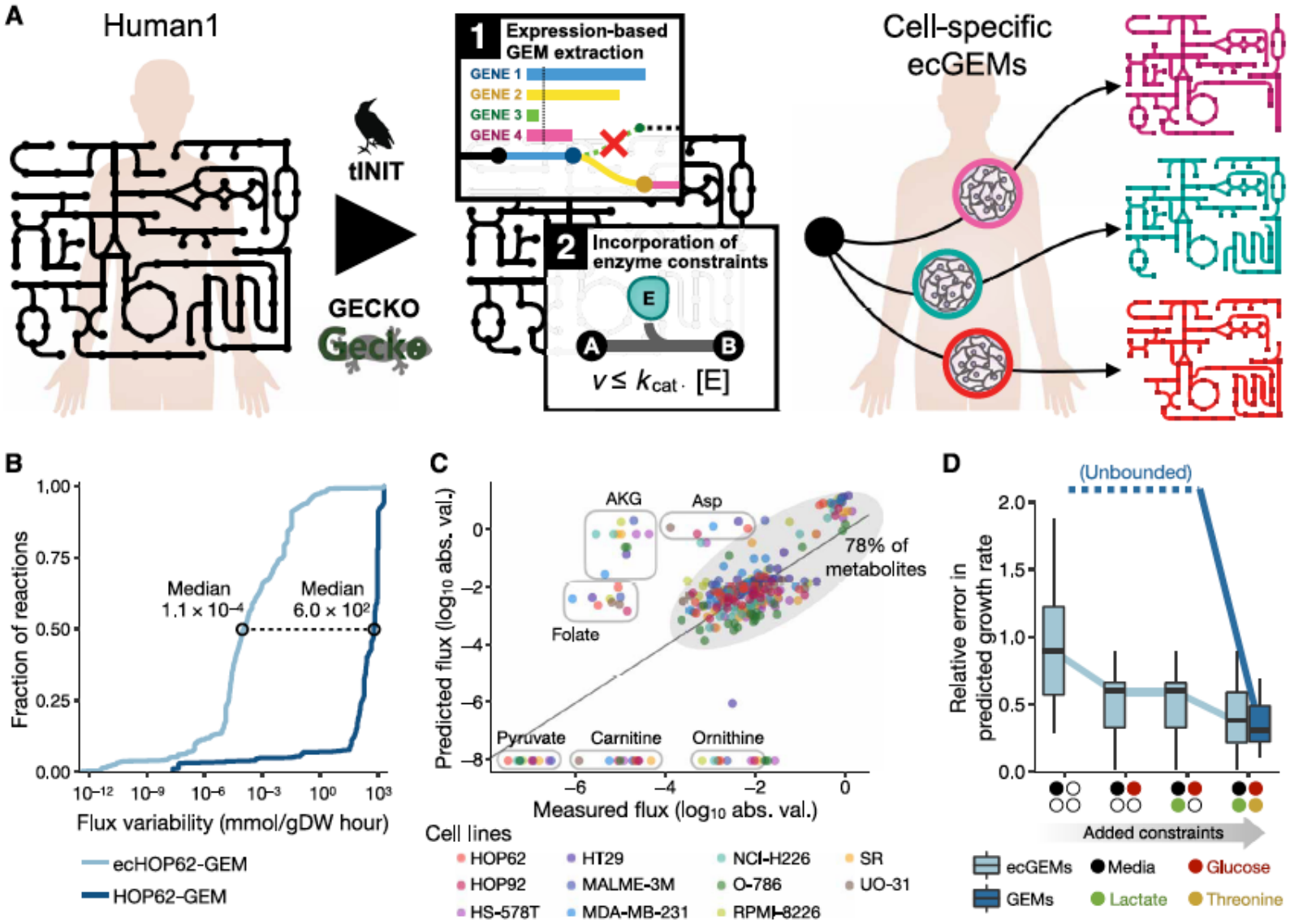
A
Human1
tINIT
GECKO
1 Expression-based GEM extraction
GENE 1
GENE 2
GENE 3
GENE 4
2 Incorporation of enzyme constraints
E
A
B
v ≤ kcat · [E]
Cell-specific ecGEMs
B
Fraction of reactions
1.00
0.75
0.50
0.25
0.00
Median 1.1 × 10−4
Median 6.0 × 102
10−12 10−9 10−6 10−3 100 103
Flux variability (mmol/gDW hour)
ecHOP62-GEM
HOP62-GEM
C
Predicted flux (log10 abs. val.)
AKG
Asp
78% of metabolites
Folate
Pyruvate
Carnitine
Ornithine
−6 −4 −2 0
Measured flux (log10 abs. val.)
Cell lines
HOP62
HOP92
HS-578T
HT29
MALME-3M
MDA-MB-231
NCI-H226
O-786
RPMI-8226
SR
UO-31
D
(Unbounded)
Relative error in predicted growth rate
2.0
1.5
1.0
0.5
0.0
Added constraints
ecGEMs
GEMs
Media
Lactate
Glucose
Threonine

Imagine taking it one step further to personalized medicine

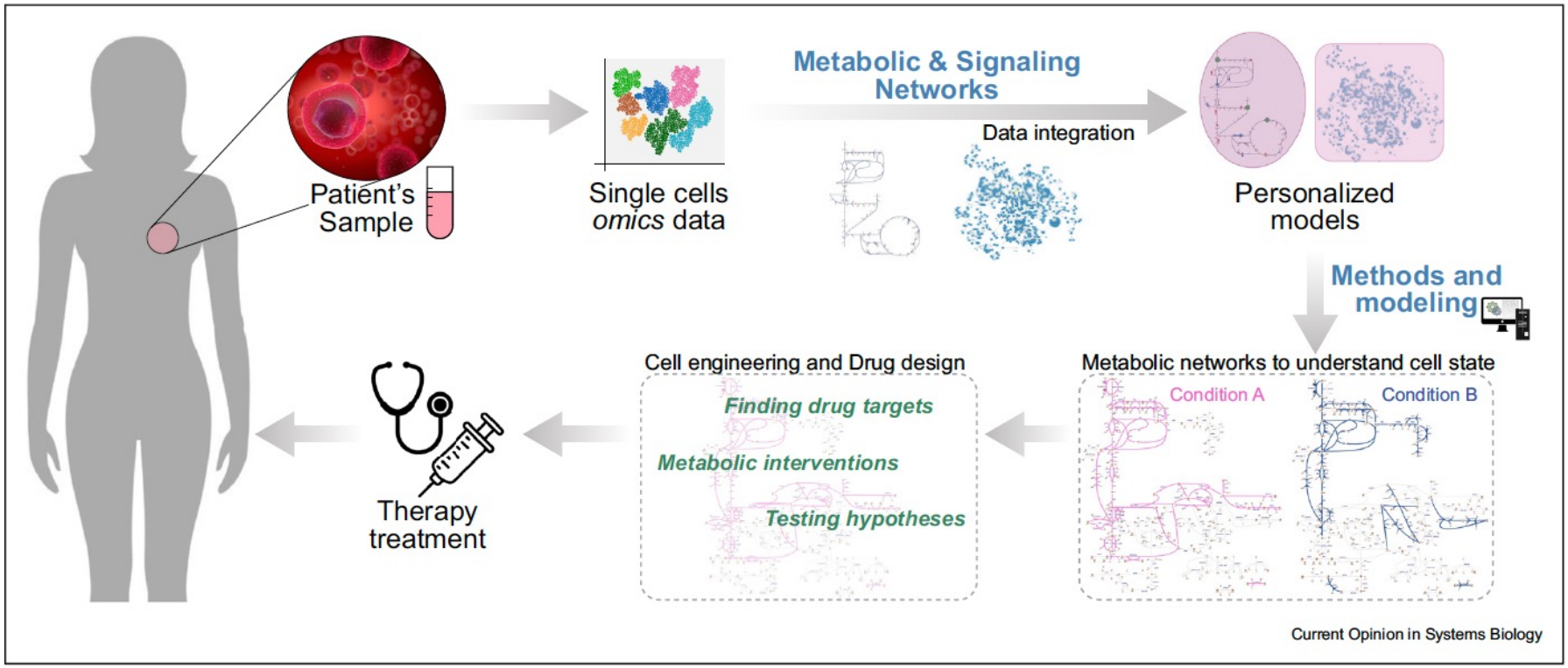

Masid and Hatzimanikatis *Curr Op Systems Bio* 2021

Memorial Sloan Kettering Cancer Center

Lets take a break and then paper discussion

Wang, M. *et al.* A wearable electrochemical biosensor for the monitoring of metabolites and nutrients. *Nat Biomed Eng* **6**, 1225-1235, doi:10.1038/s41551-022-00916-z (2022).